Centre for Geo-Information
Thesis Report GIRS-2006-25

Long-term phenology changes over the Eurasian continent using the HANTS algorithm

Diana Torres

June 2006

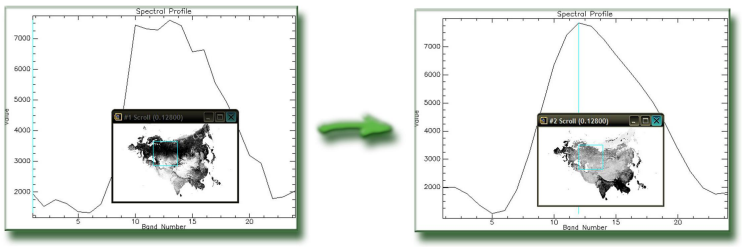

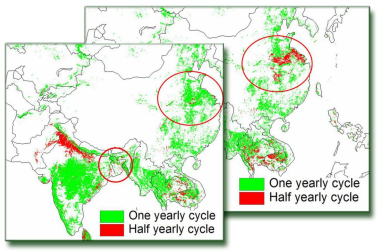

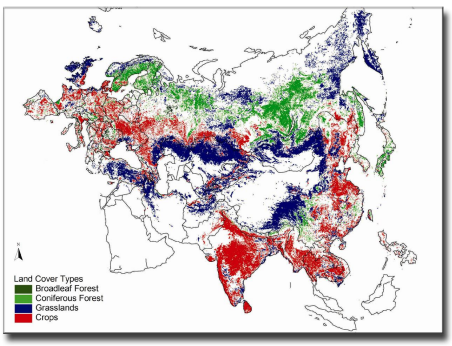

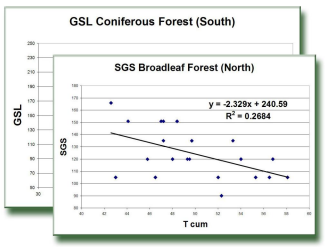

WAGENINGEN UNIVERSITY
WAGENINGEN UR

Long-term phenology changes over the Eurasian continent using the HANTS algorithm

Diana Torres

Registration number 78 06 06 840 130

Supervisors:

Drs. A. J. W. de Wit
Dr. Ir. J. G. P. W. Clevers

A thesis submitted in partial fulfillment of the degree of Master of Science at Wageningen University and Research Centre, The Netherlands.

June 2006

Wageningen, the Netherlands

Thesis code number: GRS-80436
Thesis Report: GIRS-2006-25
Wageningen University and Research Centre
Laboratory of Geo-Information Science and Remote Sensing

ACKNOWLEDGEMENT

Many people contributed in big or small ways to carry out this research. First of all I would like to thank my supervisor Allard de Wit for all his support in writing the scripts used for processing the data, his guidance and advices. Jan Clevers as my second supervisor helped me to focus the research when needed and his advices were also appreciated.

I also appreciate the advice of Arnold van Vliet about phenological data and the European Phenology Network.

My thanks go also to Michael Schaepman for the suggestions he gave to finish this thesis; Willy ten Haaf for his supervision during these 2 years of study.

I do not forget special friends who made my stay in Wageningen a nice and unforgettable time, thanks to all my classmates for everything they taught me without noticing it sometimes.

My special thanks to the Nuffic Programme for the scholarship they granted me, this experience changed my life in many ways, professionally and personally it improved my mind.

Last but not least I would like to mention the persons God gave me to make me feel support and love: my parents, family and Adam, I feel so blessed by you all. God was every step of these two years with me I could feel His hand on my shoulder...

ABSTRACT

Global warming is a phenomenon that is expected to alter the phenology of vegetation; this study was carried out in order to find the relation that the raising air temperature is having over the phenology of broadleaf forest, coniferous forest, grasslands and crops in Eurasia. Due to the big amount of satellite data to work with, and the cyclic nature of vegetation growth, the Harmonic Analysis of Time Series algorithm (HANTS) was used to analyze 21 years (1982-2002) of Normalized Difference Vegetation Index (NDVI) data from the Global Inventory Modelling and Mapping Studies (GIMMS) dataset. A Maximum Increase (MI) algorithm was used to find relevant phenological indicators: Start of Growing Season (SGS) and Growing Season Length (GSL). Air temperature from the Climatic Research Unit (CRU) dataset, and land cover data from ECOCLIMAP were also used. Trend and regression analysis were performed between phase, SGS, GSL and temperature sum of the first seven months of each year.

This study has found as result an ascending trend for the yearly sum of temperatures in the study area.

HANTS results of the amplitude showed that vegetation predominantly had a one yearly cycle behavior (one growing season per year) for all land cover classes. In the case of some areas with crops in China and Bangladesh, a change of one to half yearly cycle (two growing seasons per year) became predominant, showing that crops are being cultivated more than once a year in those areas towards the end of the 21 years.

The phase of the first harmonics could indicate changes in temperature sum for some land cover classes. From the comparisons between temperature sum and the averaged (by land cover type) phase, SGS and GSL, the results were: (1) Phase and temperature sum behave in the same way for most of the analyzed years, the trend of both curves was similar (same peeks and valleys). In the case of Coniferous Forest, this trend was not as clear as it was for the other three land cover types; (2) for SGS and temperature sum, just coniferous forest and grasslands showed a significant relationship (α=0.05) that helps us to conclude that the growing season, in the case of these land cover types, is starting earlier while the temperatures are increasing; (3) for GSL and temperature sum, the regression showed significance (α=0.05) only for coniferous forest.

From the regression analysis between temperature sum and the sample pixels (in north and south latitudes) of phase, SGS and GSL, the results showed: (1) for phase and temperature sum, northern samples for broadleaf forest and coniferous forest, and northern and southern samples of crops showed a significant correlation (α=0.05). Grasslands land cover type showed a non-significant relationship with temperature sum; (2) for SGS and temperature sum, broadleaf forest and crops (for northern pixels) were the only two land cover classes which showed significant relationships (α=0.05); (3) for GSL and temperature sum, coniferous forest (pixel in the south) was also the only land cover class which showed a significant relationship (α=0.05). The fact that seasonal temperatures instead of annual temperatures are being used could lead to poor results. The small sample size is also affecting the results of pixel samples for all the cases (phase, SGS and GSL with temperature sum).

HANTS outputs were useful to detect seasonality of the land cover classes in this study, by means of the ratio of amplitudes. The phenologic changes that are being observed as a result of global warming were also found for some land cover types using this methodology. Analyzing the relationship between phase and temperature sum we could find more significant relationships than using the phenological indicators and temperature sum. Phase could be a good indicator of temperature as a driver of changes in vegetation; however, further research could help to understand these results.

KEYWORDS: Phenology, Remote Sensing, NDVI, HANTS, Remote sensing phenological indicators.

INDEX

LIST OF FIGURES

LIST OF TABLES

LIST OF ABBREVIATIONS

AMO	Atlantic Multidecadal Oscillation
AVHRR	Advanced Very High Resolution Radiometer
CFCs	CloroFluoroCarbons
CRU	Climatic Research Group
EPN	European Phenology Network
FET	Fit Error Tolerance
FREQS	1D array with frequencies that should be selected from the Fourier spectrum. i.e. freqs = [0,1,2] to use the Fourier components 0 (mean), 1 (1 sine wave), 2 (2 sine waves)
GIMMS	Global Inventory Modelling and Mapping Studies
GS	Growing Season
GSL	Growing Season Length
HANTS	Harmonic Analysis of Time Series
IMAX	Maximum number of iterations
IPCC	Intergovernmental Panel of Climate Change
MI	Maximum Increase
NDVI	Normalized Difference Vegetation Index
NOAA	National Oceanic and Atmospheric Administration
RANGE	Array of size 2 to specify the minimum and maximum valid data values. i.e. range = [1,254]
SGS	Start of Growing Season
TAT	Throw Away Threshold
UMd	University of Maryland
VI	Vegetation Index

1 INTRODUCTION

Changes in the lengthening of the growing season, the beginning of spring and finish of autumn have raised many questions about the causes and effects of them on plant and animal populations. Several authors (Nemani et al., 2003, Zhou et al., 2001, Bogaert et al., 2002, Shabanov et al., 2002, Tucker et al., 2001) have reported the general greening up trend that the Northern Hemisphere is showing as a result of climate change. As Askeyev et al. (2005) mention, the life cycles of most plants and animals are strongly influenced by climate. Many scientists anticipate that current and future warming will alter the seasonal behavior of plants and animals. Changes are expected in phenology, in the performance of populations and in primary productivity.

Some researchers investigate this phenomenon as the result of changes in temperature due mainly to greenhouse gases emission. Increases in air temperature due to the anthropogenic greenhouse effect can be detected easily in the phenological data of Europe within the last four decades because spring phenological events are particularly sensitive to temperature (Menzel, 2000).

In Remote Sensing, analysis of Vegetation Index (VI) time-series can help to understand the behavior of plant phenology through the years. Large datasets of satellite images are available to study phenology changes but the interpretation of data to get information can be difficult; not only because of the natural variability found in the signal through years, but noise presence also adds a source of variability to data. Some mathematical techniques such as Fourier Transform proved to be an effective technique to cope with large time series images (Moody and Johnson, 2001).

Fourier or harmonic analysis is a mathematical technique to decompose a complex stationary signal into a series of individual cosine waves, each characterized by a specific amplitude and phase angle. A process that repeats itself every t seconds can be represented by a series of harmonic functions whose frequencies are multiples of a base frequency. This series of harmonic functions is called a Fourier series (Immerzeel et al., 2005). Azzali and Menenti (2000) mentioned how Fourier transformations can be useful to analyze vegetation phenology using the amplitude and phase of the most important periodic components (harmonics). Due to the cyclic

nature of vegetation growth this method will be employed to study phenology in our research area.

1.1 Problem context and definition

Eurasia, the big landmass composed by Europe and Asia is one of the most diverse areas of the world. Not only geographical, ethnic and linguistic differences are found but due to the big extension of this continent, ecosystems with completely different types of flora and fauna are present.

The present study will make use of the Global Inventory Modelling and Mapping Studies (GIMMS) normalized difference vegetation index (NDVI) dataset, that was generated to provide a 21-year satellite record of monthly changes in terrestrial vegetation (GIMMS documentation, 2005), to study this large area at a resolution of 8 km per pixel.

Since some other researchers as Azzali and Menenti (2000), Sakamoto et al. (2005), Moody and Johnson (2001) and Chen et al. (2000) have found useful Fourier methods to analyse changes in phenology, we will apply Fourier transformations, by means of the HANTS algorithm, to NDVI data of Eurasia to detect changes in phenology. This algorithm was previously used by Kross (2005) and De Wit and Su (2004) to detect changes in phenology.

A remote sensing based approach, which is spatially explicit, for monitoring climate changed is required. The present research aims to find the phenology change pattern that Eurasia is experiencing as a result of changes in climate. A pixel-based evaluation of Fourier-transformed NDVI will be done; land cover classes that match the analyzed pixels will help to explain the changes. Temperature data, as one of the most important climatological variables, will be used to investigate if changes in climate are affecting the growing season in length and start.

1.2. Research objectives

General Objective: To evaluate phenological changes over Eurasia applying HANTS to the GIMMS-NDVI dataset (1982-2002).

Specific Objectives:

- To estimate the changes in the start and length of the growing season (phenological indicators) from 1982 till 2002.
- To investigate the relation between temperature change and changes in the remote sensing phenological indicators.

Research questions:

1. How have the start and length of the growing season changed during the period 1982 – 2002 in Eurasia?
2. What is the relationship between sum of temperatures over zero centigrade degrees (January to July) and HANTS output (Phase)?
3. What is the relationship between sum of temperatures over zero centigrade degrees (January to July) and changes in phenological indicators?

1.3. Structure of this report

Chapter one of this report presents an introduction to the study topic, problem definition and research objectives.

Chapter two contains a literature review of the subjects related to this research.

Chapter three details the materials and methodology employed to carry out this research.

Chapter four exposes the results and discussion of them.

Chapter five presents the conclusions and chapter six the recommendations.

2 LITERATURE REVIEW

2.1. Climate Change

Over the 20th century the global average surface temperature has increased by about 0.6 +/- 0.2 ˚C and it is projected to continue to rise at a rapid rate (Dose and Menzel, 2004). This warming has been more intense in middle and high latitudes than in tropical areas (Xiao and Moody, 2005)

Numerous studies have been carried out in order to understand the causes and effects of climate change, which can be induced by different factors such as natural variations (internal interactions) or anthropogenic influence (external forces). Stott et al. (2000) state that "both natural and anthropogenic factors have contributed significantly to the 20^{th} century temperature changes. However, more than 80% of observed multidecadal-scale global mean temperature variations and more than 60% of 10 to 50 year land temperature variations are due to changes in external forcings".

Since the beginning of the Industrial Revolution (mid of 18th century), many changes have taken place in the composition and response of the atmosphere. Most of the changes started after the intensive use of fossil fuel (for industrial or domestic usage) and biomass burning, which produce greenhouse gases and aerosols. Emission of chlorofluorocarbons (CFCs) and other chlorine and bromine compounds has not only an impact on the radiative forcing, but has also led to the depletion of the stratospheric ozone layer. Land-use change, due to urbanization and human forestry and agricultural practices, affects the physical and biological properties of the Earth's surface. Such effects change the radiative forcing and have a potential impact on regional and global climate (IPCC, 2001).

The internal factors that cause climate change are interactions between components of the atmosphere and the ocean. For instance, El Niño-Southern Oscillation (ENSO), resulting from the interaction between atmosphere and ocean in the tropical Pacific is one of the phenomena that affect climate (Zhang et al., 2005). Sutton and Hodson (2005) state that changes in the Atlantic Ocean (Atlantic Multidecadal Oscillation

AMO) may be also an important driver of multidecadal climate variability on a global, as well as regional scale.

The summation and interactions between anthropogenic and natural factors, which affect climate, have produced several different phenomena in climate variables (raising temperatures, scarce precipitation, etc) that can be observed nowadays. Understanding of climate behavior, the past and present, will help to predict future states of climate in order to support policymakers to plan tasks in agriculture and other fields of economic development.

2.2. Phenology Changes related to changes in climate

Phenology is the study of the timing of recurrent biological events and the causes of timing with regard to biotic and abiotic forces (Lieth, 1975 quoted by Botta et al., 2000). Dose and Menzel (2004) state "phenology is perhaps the simplest and most frequently used bio-indicator to track climate changes".

"In recent years, determining the growing season of land vegetation on a large scale has become an important scientific question for research into global climate change" (Chen et al., 2000). Climate change can also be affected by land use changes happening to a more intensive degree nowadays. Feddema et al. (2005) have analyzed the relation between land cover change and climate change, finding that choices humans make about future land use could have a significant impact on regional and seasonal climates. For instance, urban areas locally increase evening springtime sensible heat that could be detectable in phenology (Fisher et al., 2006).

Menzel (2003) gathered information from earlier observations of relationships between climatic variables and phenology, "Seyfert (1955) observed that warm weather situations induced earlier onset of spring and summer phases, whereas in autumn phenological phases are delayed by warmer periods. Mahrer (1985) tested this hypothesis for two sites in Switzerland and found warmer autumn temperatures delaying leaf coloring. And similar to the results presented here, he found that spring temperatures enhanced leaf coloring at these two sites".

Several studies have been carried out to analyze the effects of climate variable changes (temperature, precipitation, etc) on phenologic stages. Changes in climate have caused variations in life cycles of many plants and animals. Several scientists anticipate that current and future warming will alter the seasonal behavior of plants and animals. Changes are expected in phenology, in the behavior of populations and in primary productivity (Askeyev et al., 2005). Spring phenological events are particularly sensitive to temperature, for instance in the research made by Menzel (2000) covering 40 years, leaf unfolding has advanced on average by 6.3 days, whereas autumn events, such as leaf coloring, have been delayed on average by 4.5 days (+0.15 day/year). Menzel and Fabian (1999) reported an advance in the seasonal cycle of about 7 days that was inferred from CO2 data taken between the 1960s and early 1990s, with most of the effect occurring after 1980. Dose and Menzel (2004) observed advancing of flowering and leaf unfolding in Europe and North America by 1.2–3.8 days per decade on average, and a strong seasonal variation with highest advances in early spring. Zhou et al. (2001) concluded that the duration of the active growing season increased by about 18 ± 4 days in Eurasia.

One of the most important climate variables that affect phenology is temperature. Xiao and Moody (2005), Zhou et al. (2001), Myneni et al. (1997) and Keeling et al. (1995) to cite some, concluded that the active growing season has been influenced by changes in temperature as a result of global warming. To correlate the behavior of temperature to the one of vegetation can give us insights in one of the causes of the changes on vegetation that have been found lately.

2.3. Remote Sensing Phenological Indicators

Climate is the main variable that controls leaf phenology for a given biome at a global scale, and satellite observations provide a unique means to study the seasonal cycle of canopies (Botta et al., 2000)

Phenological phases obtained from measurements done in the field and standardized by the European Phenology Network (EPN) are:

SL	Sprouting of leaves
UL	Beginning of unfolding of the leaves, 1st leaf surface visible
BF	First flowers open. Beginning of flowering / of blossom
FF	Full flowering / General flowering / Full blossom
EF	End of Flowering / of blossom
RP	Fruit ripe for picking (pome fruit, sweet cherry, morello and currant)
RP	First ripe fruits (European chestnut, almond)
CL	Coloring of leaves
FL	Leaf fall

Source: EPN http://www.dow.wau.nl/msa/gpm/, 08/02/2006

These phenological phases cannot be detected by remote sensed data, so the remote sensing phenological indicators are simplified to: Start of Growing Season (SGS), End of Growing Season (EOS) and Growing Season Length (GSL). Shifting of SGS gives an indication of changes of the beginning of growing season (GS) along the years. Schwarz and Reiter (2000) state that phenological indicators as leaf appearance or flower bloom in plants can serve as convenient markers to monitor the progression of the yearly shift on the beginning of the growing season, and assess long-term changes resulting from climate variations.

Kross (2005) compared two methods, Seasonal Midpoint NDVI (SMN) and Maximum Increase (MI), to obtain remote sensed phenological indicators, finding no big difference among them. The MI method, as defined by De Wit and Su (2004), states that the smoothed NDVI profile obtained after the application of the HANTS algorithm provides a useful way to calculate derivatives afterwards. The start of growing season was defined as the point in the year with the largest positive rate of change (maximum of first derivative), and the end of the growing season as the point in time where the NDVI drops below the NDVI at the start of the growing season. This method has been successfully applied by the authors mentioned above, finding results consistent with records of the beginning and end of the growing season for the different species in study.

2.4. Harmonic Analysis and HANTS algorithm

In large datasets of satellite images, interpretation of data to get information can be difficult; not only because of the natural variability found in the signal through years, but noise presence also adds a source of variability to data. Long time series of data require methods to make them readable and understandable.

A process that repeats itself can be analyzed by a series of harmonic functions whose frequencies are multiples of a base frequency. This series of harmonic functions is called a Fourier series. In other words, what Fourier or harmonic analysis makes is to decompose a complex static signal into a series of individual cosine waves, each characterized by a specific amplitude and phase angle (Immerzeel et al., 2005).

In the research done by Azzali and Menenti (2000) it is explained that amplitude values for periods of twelve months are closely related to biological phenomena, "such as the growth of vegetation in response to the annual patterns of temperature and rainfall. The amplitude at one year period measures the maximum variability of the NDVI values over one year, from the minimum to the maximum NDVI values. The phase value at one year period is the time lag between the maximum NDVI and the beginning of the series."

The HANTS algorithm performs a Fourier analysis on time series (e.g. NDVI images) and determines the amplitude and phase of the most significant frequencies (Mücher et al., 2002). This algorithm, previously used by Kross (2005), De Wit and Su (2004) and Roerink et al. (2000) to detect changes in phenology (the first two articles), and to reconstruct cloudfree NDVI image composites, have shown interesting results so far. HANTS is considered to be a robust fast smoother.

3 MATERIALS AND METHODS

3.1. Study area

Eurasia comprises Europe and Asia which were politically divided in the past although they are part of the same land mass. Koulakov (1998) mentions the separation that the Indian plate and the Eurasian continent had in the past, although tectonically these areas are not from the same origin. In this study we will consider Eurasia as the big land mass composed by Europe and Asia including India. In figure 3-1 this continent appears in green. Our study is focused on this continent, taking into account four land cover classes.

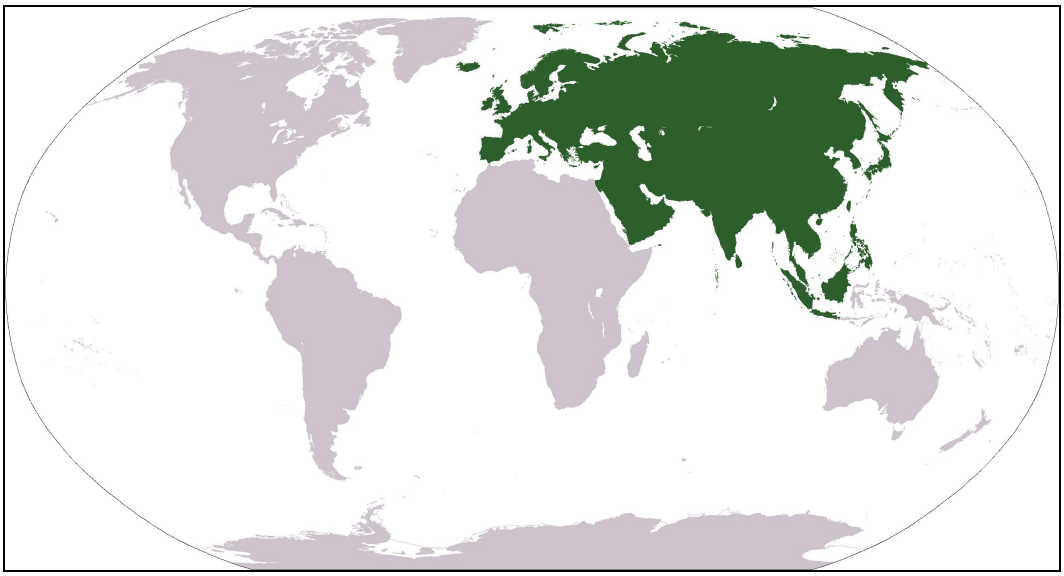

Figure 3-1. Location of Eurasia in the world.
http://commons.wikimedia.org/wiki/Eurasia (last modified: 29 March 2006)

Figure 3-2 shows the four vegetation classes in study: broadleaf forest (138 304 km^2), coniferous forest (3 113 792 km^2), grasslands (5 959 744 km^2) and crops (5 526 464 km^2). The first three land cover classes were selected due to their importance to detect phenology changes. The crop class was also evaluated to observe some changes in farmer decisions through the years of climate change.

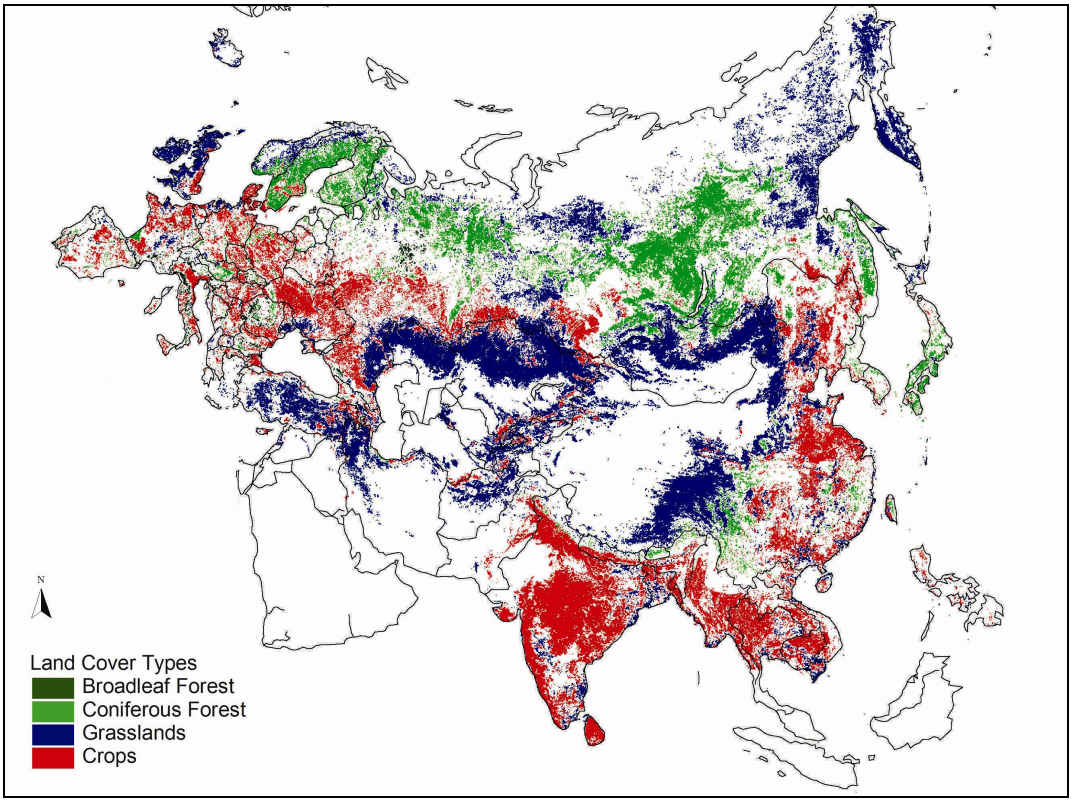

Figure 3-2. Land cover classes in Eurasia from ECOCLIMAP

3.2. Datasets

3.2.1. Remote sensing data

The remote sensing data used for this study was produced by the Global Inventory Monitoring and Modeling Studies (GIMMS). The GIMMS normalized difference vegetation index (NDVI) data sets were generated to provide a 21-year satellite record of monthly changes in terrestrial vegetation (GIMMS, 2005). The Eurasia subset at 8 km resolution for the period January 1982 to December 2002 was obtained.

NOAA-AVHRR data were used to derive NDVI images. NDVI is the difference (in reflectance) between the AVHRR near-infrared and visible bands divided by the sum of these two bands (Lillesand et al., 2004).

Some useful characteristics of the GIMMS NDVI dataset:

Parameter/ Variable Name	Parameter/ Variable Description	Data Range	Units of Measurement	Data Source
GIMMS NDVI	Normalized Difference Vegetation Index calculated from AVHRR channel 1 and 2 digital count data.	Theoretical range between -1 and 1; values around 0 for bare soil (low or no vegetation) values of 0.9 or larger for dense vegetation.	[Unitless]	AVHRR

3.2.2. Land cover data

ECOCLIMAP is a global dataset at a 1km resolution. This dataset has fifteen land cover classes, which were derived with the help of the University of Maryland (UMd) global land cover map. The classes are: evergreen needleleaf forest, evergreen broadleaf forest, deciduous needleleaf forest, deciduous broadleaf forest, mixed forest, woodland, wooded grassland, closed shrubland, open shrubland, grassland, cropland, bare soil, urbanized areas, permanent snow and ice, and wetlands. In Europe, 3 major forest types (broadleaf, needleleaf, and mixed) were obtained as output (Masson et al., 2003).

Broadleaf and coniferous forest classes and grasslands were chosen to work with in the detection of phenologic changes. Crop class was also chosen to compare natural vegetation with this man-managed type of vegetation.

3.2.3. Climate data

High resolution (0.5˚) mean temperature data from the Climatic Research Unit (CRU) group was obtained in order to use for validating remote sensing phenologic indicators. This dataset was generated as a product of climate field data that was interpolated as a function of latitude, longitude and elevation using thin-plate splines. Nine variables: precipitation, wet-day frequency, mean temperature, diurnal temperature range, vapor pressure, sunshine, cloud cover, ground frost frequency, and wind speed were derived (New et al., 1999). From that dataset, mean temperature was chosen.

3.3. Methodology

The overall methodology employed can be divided in the main three blocks of data processed and analyzed. NDVI data from GIMMS, four land cover classes (broadleaf forest, coniferous forest, grasslands and crops) from ECOCLIMAP, and mean temperature from the CRU dataset are the three types of data used (see figure 3-3).

3.3.1. Processing of NDVI data

One GIMMS NDVI stacked file was obtained, containing 21 years of data, 2 bands per month and coverage of the whole world.

- Spectral Subsetting

Each year, composed by 24 bands (15-day composite), was extracted to work year by year.

- Application of HANTS

The HANTS algorithm was employed to smooth the dataset. HANTS was applied in the same way Kross (2005) and De Wit and Su (2004) used it. As Kross (2005) described, this algorithm needs five parameters to be set: RANGE, FREQS (frequencies), IMAX (Maximum number of iterations performed during processing), FET (Fit Error Tolerance) and TAT (Throw away threshold, the maximum number of NDVI observations that can be discarded in the fitting process). The RANGE parameter is between minus one and one because the NDVI values are in this range. FREQS were set as [0,1,2] and they refer to the frequencies in the signal we want to extract; 0 refers to the mean, 1 and 2 are referred to the sine waves 1 and 2.

In this research, the input parameters were set as:

FET = 2000 (value equivalent to 0.2 of NDVI value) set by the analysis of a sample of 25% of the years in study finding a standard deviation of 0.2 on average.

FREQS = 0,1,2,3

TAT = 8 (1/3 of 24 images per year)

RANGE = -10000, 10000 (equivalent to -1 and 1, the range of NDVI)

IMAX = 10

- Calculation of Phenological Indicators

To find the start and end of the growing season in one year of HANTS smoothed NDVI time-series, a MI algorithm was applied. As De Wit and Su (2004) say, smooth NDVI profiles are convenient for calculating derivatives. Start of growing season is found by searching for the maximum of the first derivative. End of season is found by searching for the point where the NDVI drops below the NDVI at the start of the season.

The GSL is calculated by subtracting the SGS from the EOS. A conversion to days is made because these phenological indicators are given as number of temporal intervals (15 days each).

As shown in figure 3-4, after the application of HANTS on the GIMMS-NDVI dataset, two sub-products are useful for the next processing steps. The SMOOTHED data and the HANTS COMPLEX data are the inputs to find the Remote Sensing Phenological Indicators and relevant Amplitude and Phase per year, respectively.

The MI algorithm is applied to SMOOTHED data to obtain the Start and End of Growing Season. By the subtraction of SGS from EOS the GSL could be found. Statistics of these images are obtained by land cover type.

- Spatial aggregation of HANTS output (to 0.5 °)

The HANTS complex data is aggregated over the CRU grid, and an average of these complex values is calculated over a number of pixels that match each CRU grid pixel (resolution of 0.5°). Amplitude is calculated by means of the ABS function, which returns absolute values or their magnitude from complex numbers. Phases are obtained using the ATAN function, which returns the angle, expressed in radians from complex data. Amplitudes and Phases are calculated per year and land cover type. Statistics from the band corresponding to Phase 1 was obtained (Figure 3-4).

The amplitude results were used to find the behavior of the different types of land cover. Amplitude number one belongs to the first harmonic extracted by HANTS, and amplitude number two to the second harmonic.

A pixel with high amplitude 1 means a pixel with a high value for the first harmonic and one yearly cycle behavior consequently. Half yearly cycle behavior is given in pixels with high value of amplitude 2.

After applying HANTS each pixel has both values of amplitude in high or low proportion. The ratio between Amplitudes 1 and 2 (A1/A2) was obtained in order to find the yearly behavior (one or half yearly cycles) from the pixels under study. Pixels with ratio up to 1 present half yearly cycle behavior due to high values of Amplitude 2 and consequently high values of second harmonic. Pixels with ratio values over 1 have one yearly cycle behavior because of high values of Amplitude 1 and high values of first harmonic.

3.3.2. Processing of CRU data

Three mean temperature stacked images were obtained, the first one containing years 1982-1990, the second one 1991-2000 and the third one 2001-2002. A subset of each year with 12 bands per year (one per month) was obtained.

- T sum per each year

Figure 3-5 shows the processing of the CRU data. Pixel values greater than zero are obtained per month in order to sum these values for the first seven months each year. This dataset is used later in the analysis stage.

Masks with the pixels containing values of Phase 1 were built per year and land cover type in order to obtain statistics of temperature sum per land cover type and year. Masks of values non equal to zero are obtained. These masks were applied to the temperature sum image per year in order to obtain the temperature per land cover type on the pixels which will match later their geographically similar pixels of phase and phenological indicators.

3.3.3. Processing of Land cover data

- Calculation of land cover class percentage per GIMMS pixel

The Ecoclimap dataset has a resolution of 1 km per pixel. To rescale this dataset to the 8 km resolution of the GIMMS dataset, a majority fraction calculation of land cover classes was done on pixels that would match each GIMMS pixel in order to obtain pixels of 8 km resolution and the percentages of land cover present in each one.

- Clipping of relevant land cover classes

Clipping land cover was based on 70% abundance of land cover per pixel: four land cover classes were chosen as interesting to work with, broadleaf forest, coniferous forest, grasslands and crops. A subset of all pixels that showed over 70% of purity of each class was done for all the land cover classes in this study.

3.4. Analysis

Trend Analysis

After obtaining the descriptive statistics for the phenological indicators (GSL and SGS) and phase 1, the mean of these variables per year and land cover type were plotted against the mean of temperature sum per year.

Trends between both, the phenological indicators and phase 1 with temperature sum were analyzed. Due to time constrain averaging by land cover types was done.

Regression Analysis

Regression analysis was performed in the sample pixels taken in North and South areas per land cover type (see table 3-1) between:

- The phenological indicators (GSL and SGS) and temperature sum
- The phase 1 and temperature sum.

	North Sample Pixel	South Sample Pixel
Broadleaf forest	59°15' N/47°15' E	44°15' N/5°45' E
Coniferous forest	63° 45' N/18°15' E	27°15' N/100° 15' E
Grasslands	62°15' N/149°45' E	12° 45' N/79°45'E
Crops	50° 15' N/20°45' E	24° 15' N/79° 45' E

Table 3-1. Location of pixel samples per land cover type

Values of R^2 and Pearson correlation were analyzed for each regression performed.

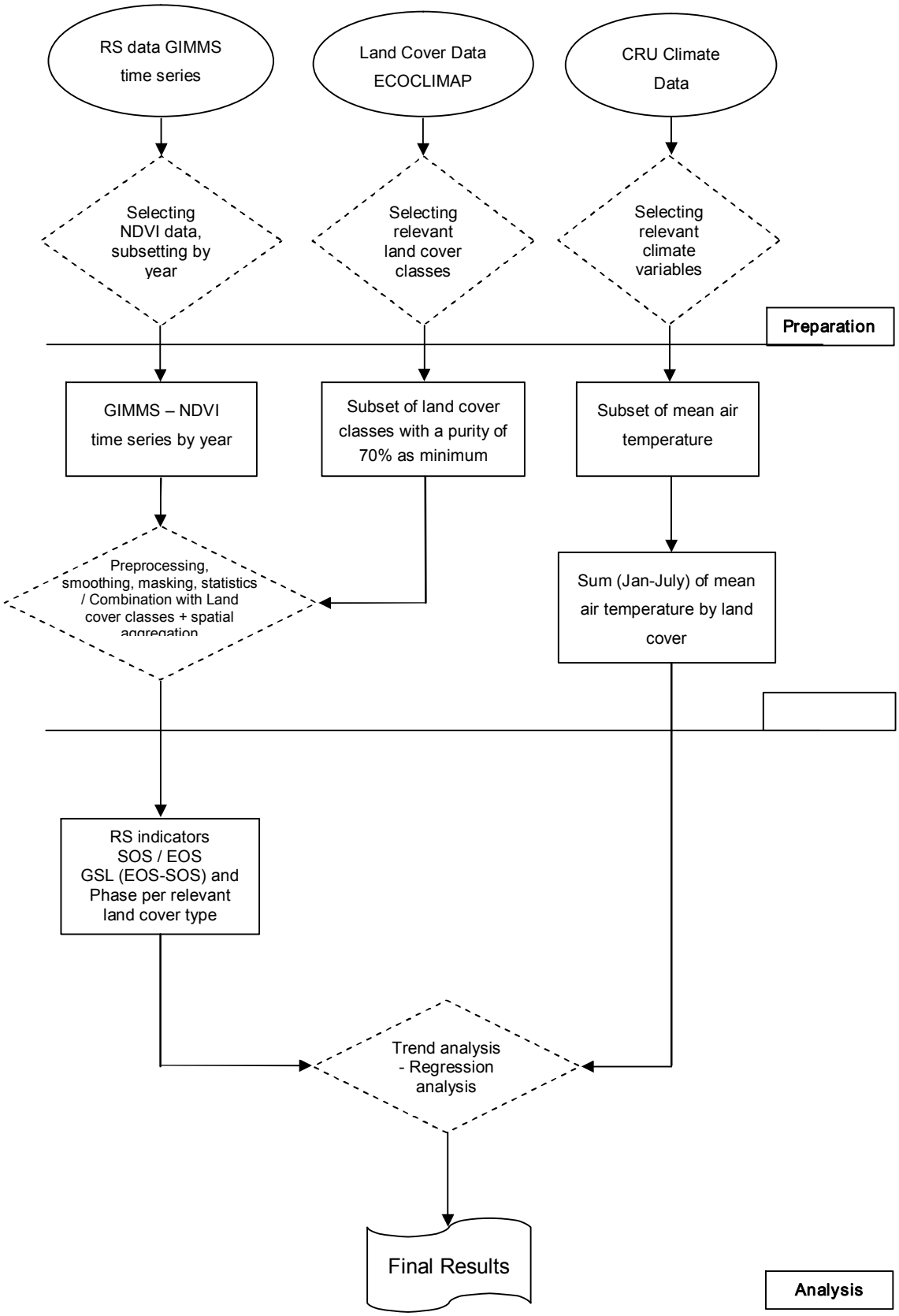

Figure 3-3. Overall methodology

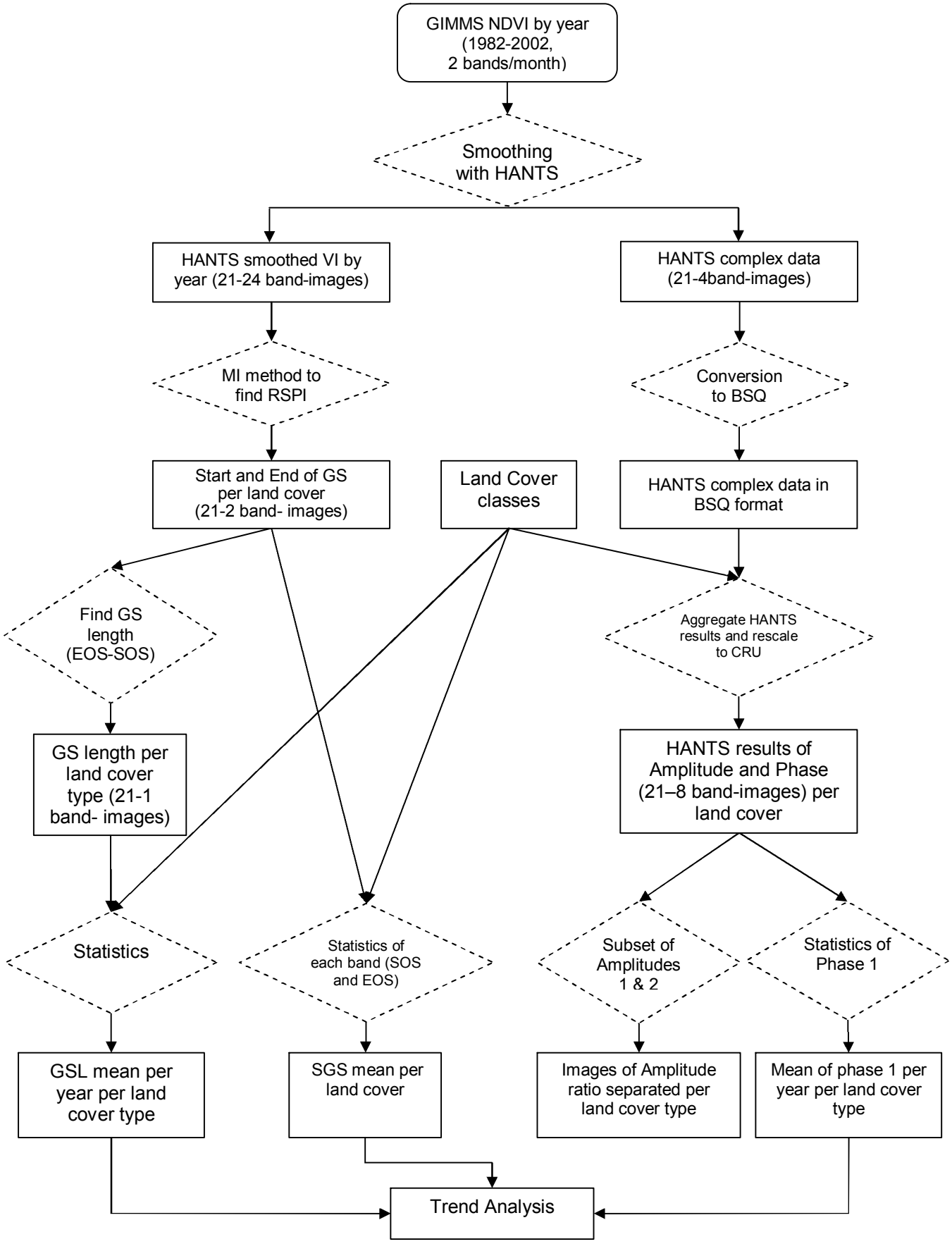

Figure 3-4. Detailed overview of GIMMS NDVI processing

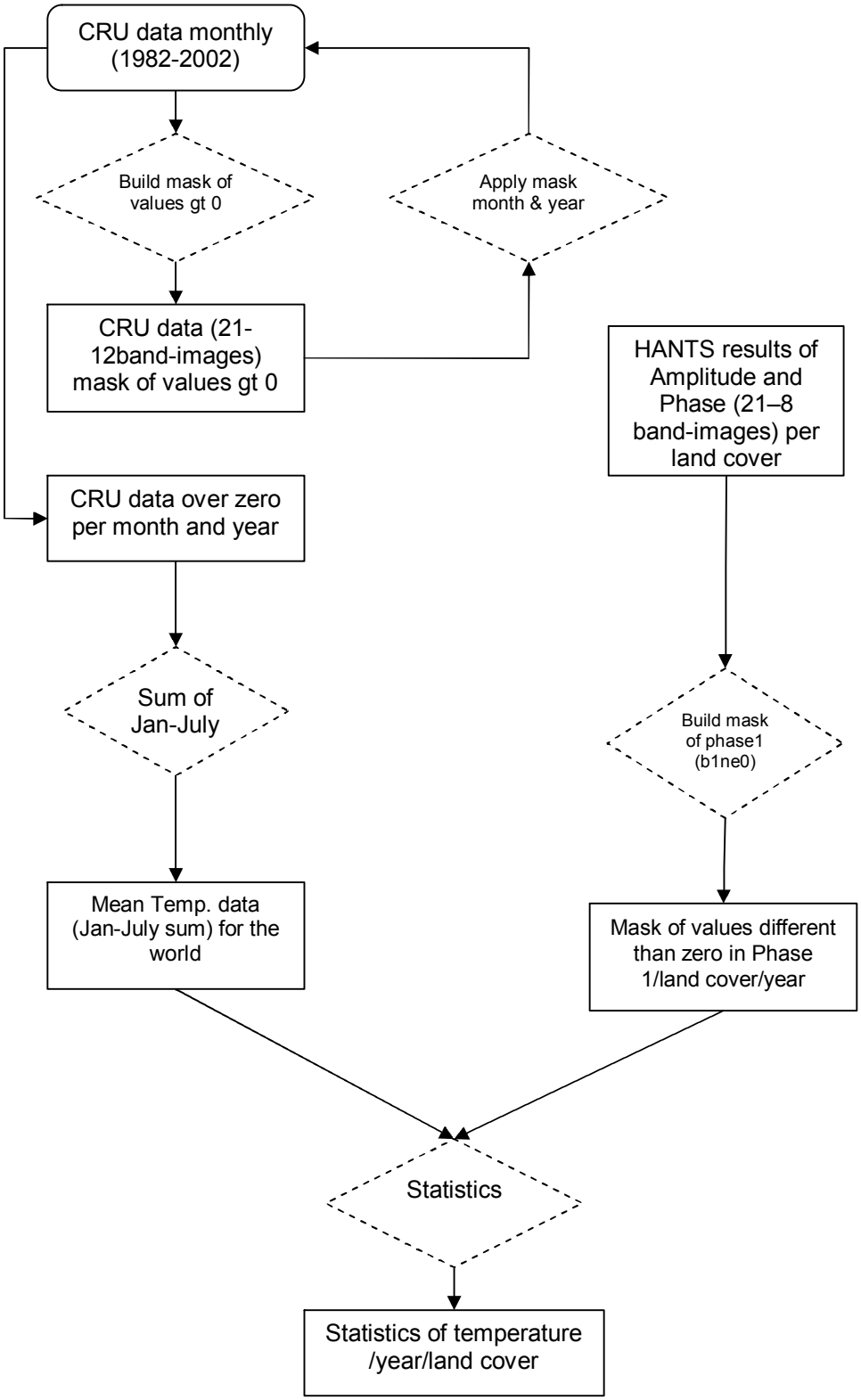

Figure 3-5. Overview of processing methodology of the CRU data

4 RESULTS AND DISCUSSION

4.1. Temperature time series

Many researchers (e.g. Zhou et al., 2001, Dose et al., 2004) have found a clear warming trend in global temperature. In figure 4-1, results of CRU data analyzed for pixels in Eurasia that match with the four land cover classes in this study are given. Mean temperature over zero degrees for January to July were summed. The accumulated temperature shows a clear ascending trend and a difference of more than 6 ˚C between the average temperature sum in 1982 and 2002.

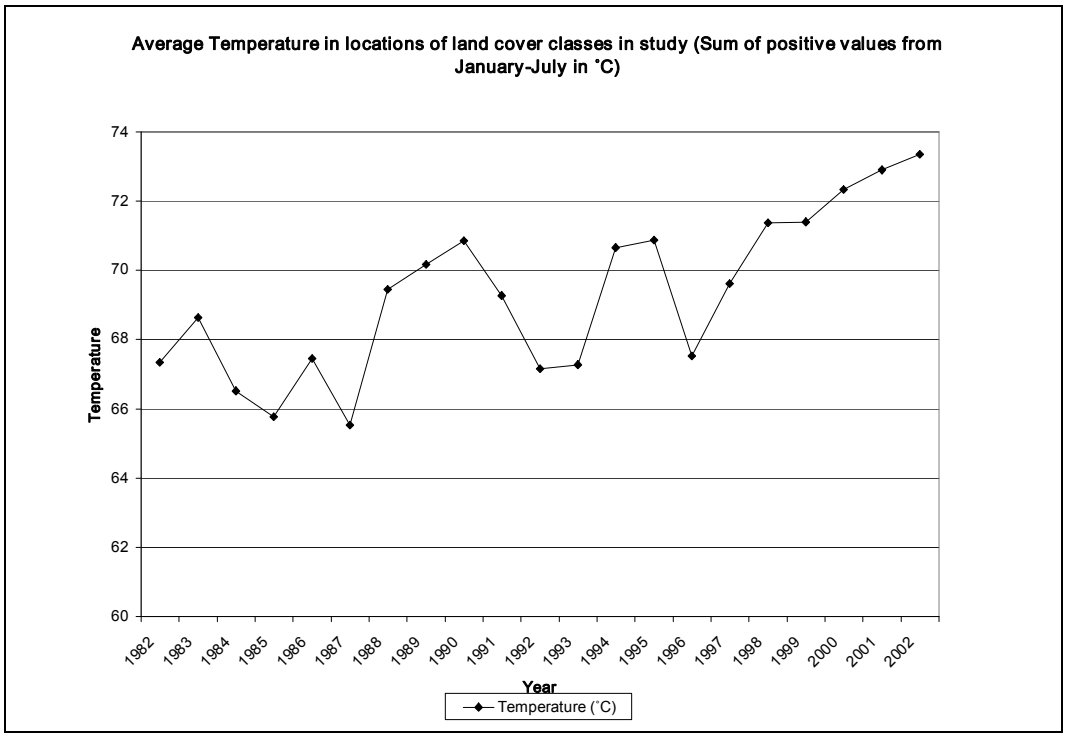

Figure 4-1. Mean Temperature averaged over all land cover types.

In the early 1914, Shreve mentioned the importance temperature had on the type of vegetation growing on a determined place. As shown in figure 4-2, crops grow in areas with higher temperatures than the other vegetation types. Coniferous forest, mainly due to its composition by trees which grow under freezing temperatures, is the land cover type in places with the lowest temperatures. Grasslands grow also in areas with a low average temperature. Broadleaf forest appears to grow in places with higher temperatures than grasslands and coniferous forest.

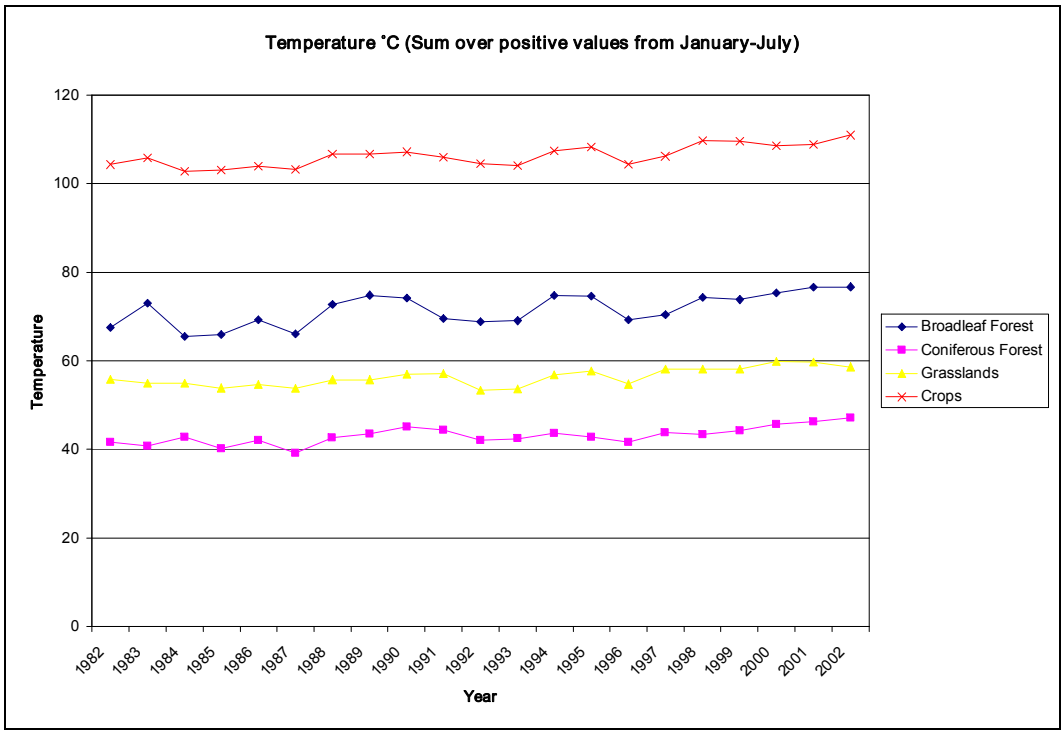

Figure 4-2. Mean Temperature by land cover type

4.2. Hants results

4.2.1. Spatial distribution of amplitude of NDVI to find yearly and half yearly cycles

Amplitude as one of the results given by HANTS will explain which harmonic (1 or 2) shows a higher value, therefore more presence of a given harmonic in the decomposed signal of NDVI. When the first harmonic predominates, we are dealing with one growing cycle per year. When the second harmonic is more dominant, we have two growing cycles.

All land cover classes showed a dominant one yearly cycle behavior (pixels in green). As shown in figures 4-3, 4-4 and 4-5 the predominant behavior is one yearly cycle for broadleaf and coniferous forests and grasslands.

In figure 4-5 there are some pixels that appear in red: some species considered inside the grasslands vegetation type must have a two yearly cycle behavior. In the first two cases for forests, almost no pixels showing this behavior appear; probably the few pixels of this type are some errors that came out after HANTS due to clouds or some other sources of error during the acquisition of the satellite image.

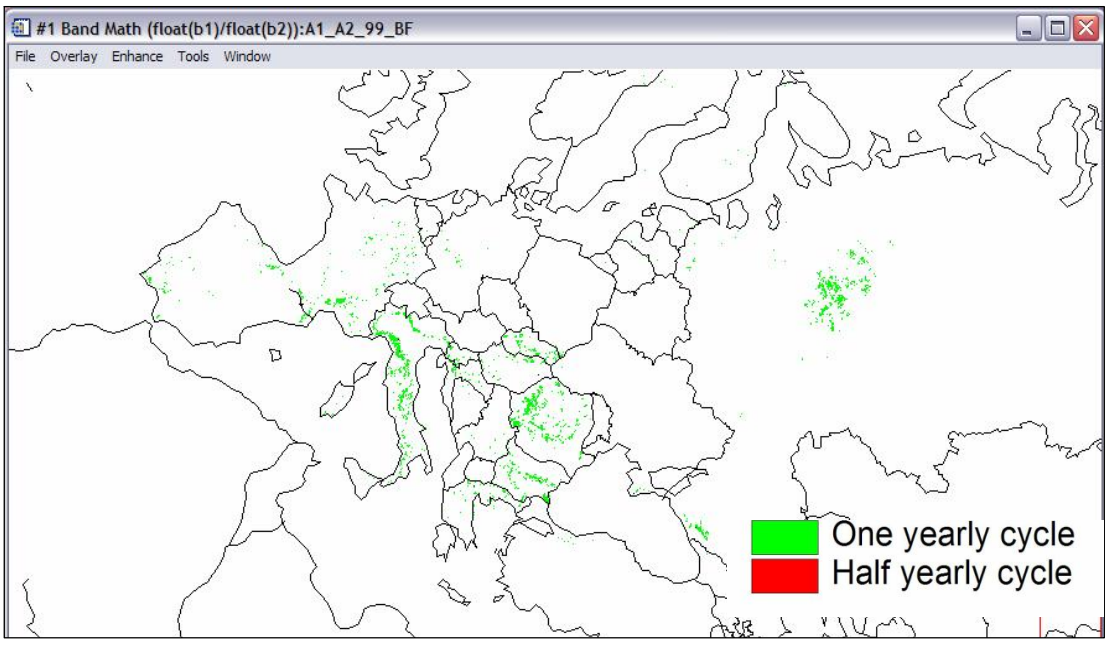

Figure 4-3. Spatial distribution of dominant one and half yearly cycles for broadleaf forest

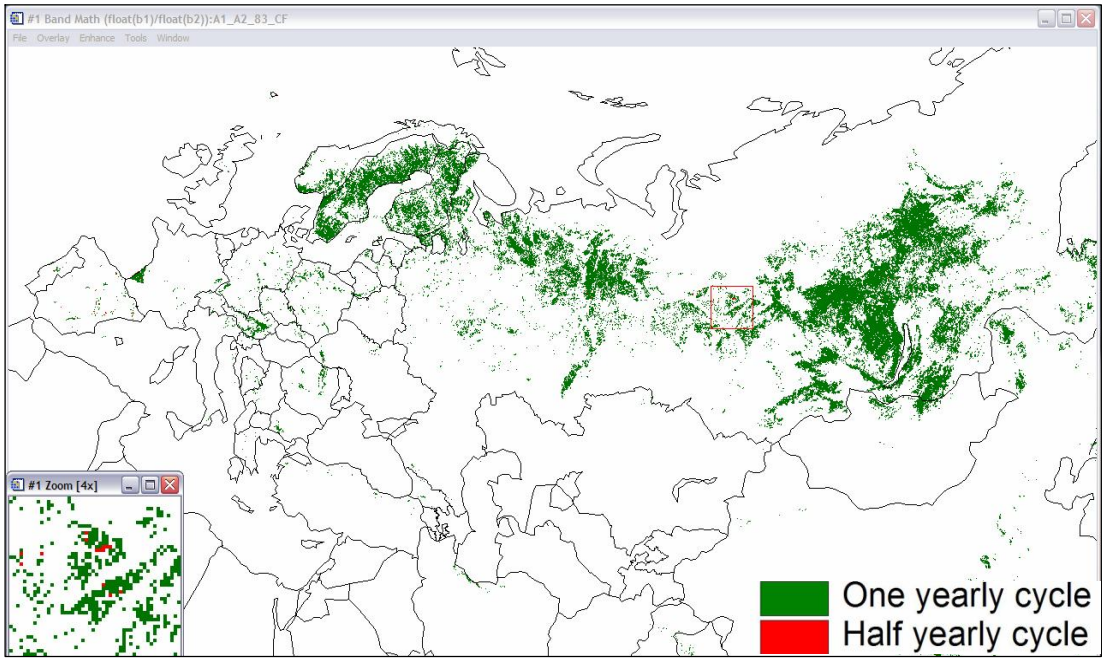

Figure 4-4. Spatial distribution of dominant one and half yearly cycles for Coniferous forest

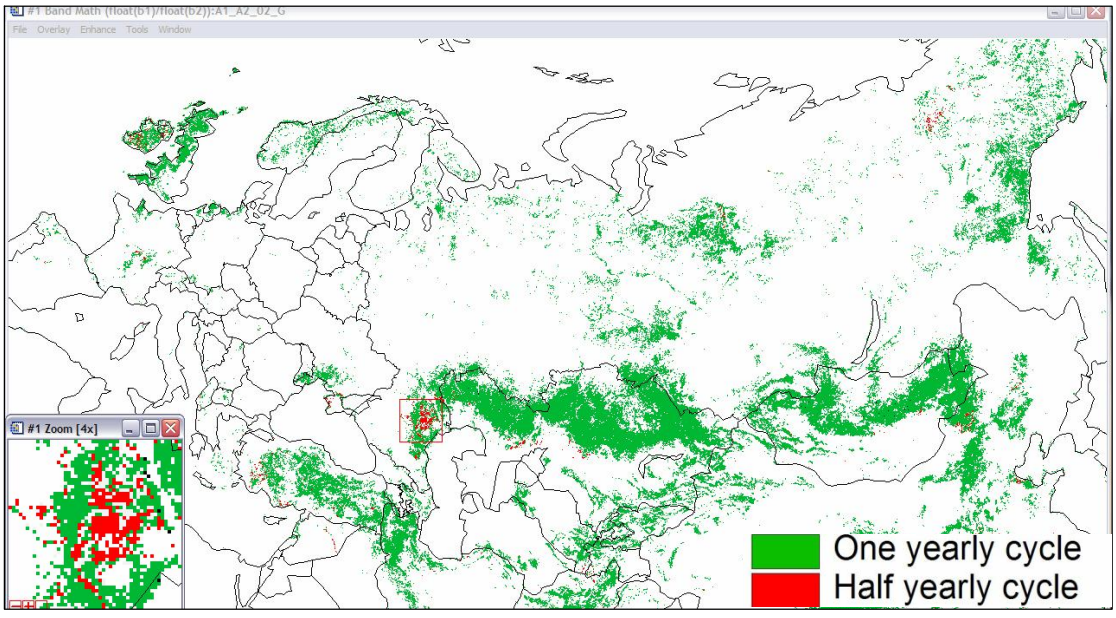

Figure 4-5. Spatial distribution of dominant one and half yearly cycles for Grasslands

In figure 4-6 and 4-7 for the land cover crops, it is noticeable that after 21 years, the area of pixels with a half yearly cycle behavior has increased in the places inside red circles. The areas which are being cultivated twice a year are increasing.

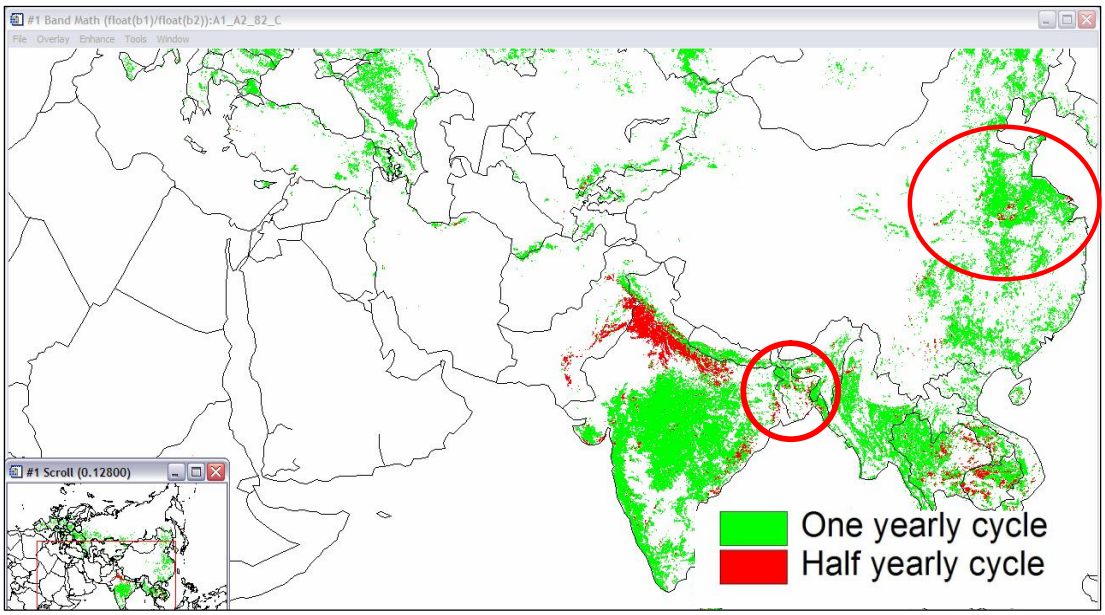

Figure 4-6. Spatial distribution of dominant one and half yearly cycles for Crops (1982)

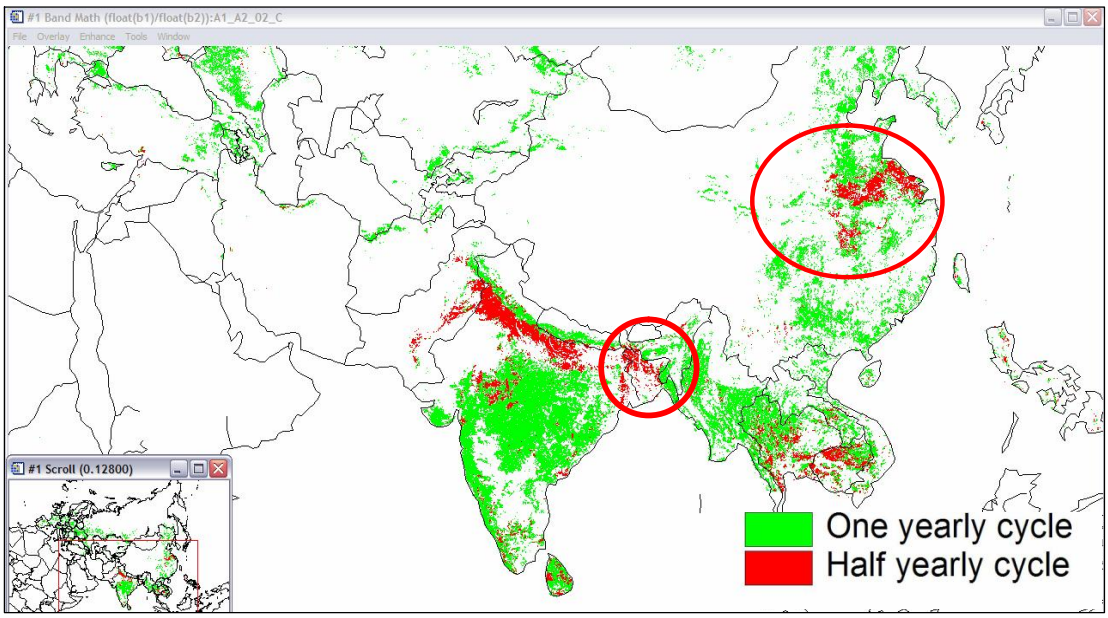

Figure 4-7. Spatial distribution of dominant one and half yearly cycles for Crops (2002)

Discussion

The amplitude obtained by the HANTS algorithm can be useful for several purposes. For instance by direct calculation of the ratio of the amplitudes (of first and second harmonics), it is possible to detect which pixels show a one yearly cycle or half yearly cycle behavior. For all the vegetation types under study the one yearly cycle behavior is dominant. In the case of crops, two areas show a visible change from one to half yearly cycle behavior in 21 years, East China (mainly Jiangsu Province) and Bangladesh.

In the Chinese area of Jiangsu, double cropping systems that consist of either winter wheat and paddy rice or rapeseed and paddy rice dominate the area (Xiao et al., 2002).

Bangladesh has been studied due to the problems caused by deforestation, erosion and low soil fertility. Islam et al. (2005) says that many big companies grew due to the production of crops like tea, rubber, pineapple, jackfruit etc destroying hills. In this form of destruction, they are mostly destroying the forest over the hills, and planting it with different crops.

Prasad et al. (2003) say that forest cover in India has been cut for shifting cultivation as one of the main purposes. A change to intensive cultivation in these areas, due to population growth and industrial development has taken place in many parts of Asia.

4.2.2. Phase of first harmonic per land cover type and year

Due to the high abundance of the first harmonic in all land cover types, only phase 1 (corresponding to this harmonic) was plotted in this section, for all the averaged sample pixels per land cover type.

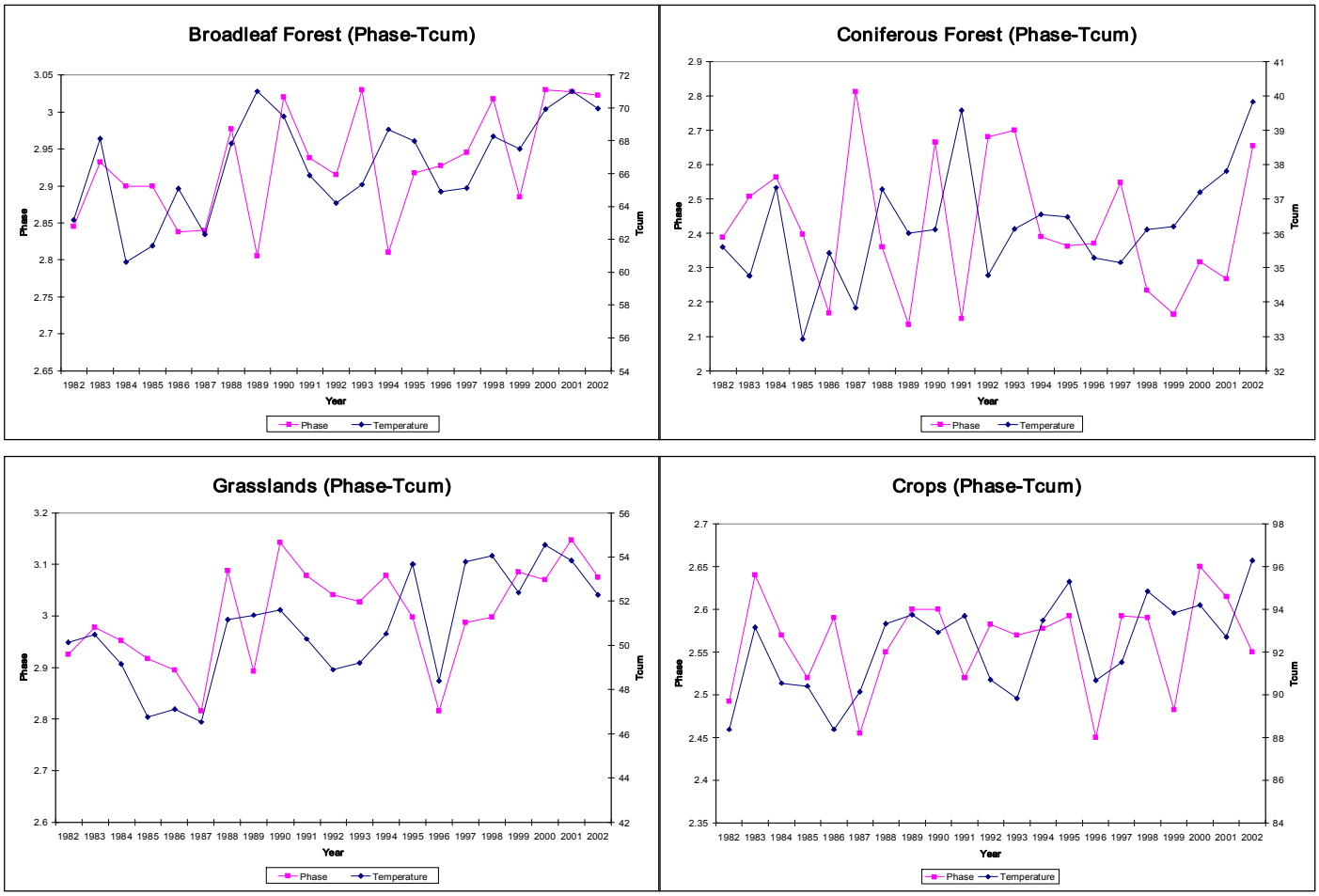

Figure 4-8. Averaged sample pixels of phase 1 and cumulative temperature (Tcum) per land cover type.

As shown in figure 4-8, phase 1 per land cover type and temperature sum (Tcum as named in the graphs) present in most of the cases a similar trend (the same peeks and valleys along the curves) for almost all the years.

Grasslands land cover is showing that phase 1 behaves similarly to temperature sum for those averaged pixels, only year 1989 presents an opposite behavior of both curves (phase and temperature sum).

For broadleaf forest, years 1985, 1986, 1989 and 1994 are the only ones which present an opposite behavior between phase 1 and cumulative temperature. For crops seven years (1986, 1987, 1990, 1991, 1992, 1998 and 2002) have a different trend, while 14 years have the same trend between phase 1 and cumulative temperature.

In the case of coniferous forest, 12 years (1983, 1986-1988, 1991, 1992, 1994, 1996-1999 and 2001) have opposite trends between the plotted variables, being the land cover class with most differences between phase 1 and temperature sum.

Discussion

Azzali and Menenti (2000) say the results of phase at different frequencies are a measure of the response of vegetation to weather.

If global warming causes spring to start earlier, year by year the phase should be larger. However, it is not clear from figure 4-8 if this type of shift exists due to short ranges of phases found for each land cover type for the 21 years. If there is a similar trend between phase and temperature sum, a regression analysis will help to explain this relationship.

4.3. Remote sensing phenological indicators

4.3.1. Start of growing season

In order to see if the growing season is starting earlier year by year, we obtained the start of growing season per pixel as a remote sensing phenological indicator on a yearly basis. Relating this change to changes in temperature will help us to understand if global warming could be one of the reasons for an earlier spring.

As shown in figure 4-9, all types of vegetation have a trend to start the growing season earlier, the negative slope in all the cases supports this statement.

However, only the trendlines for coniferous forest and grasslands have a significant R^2 (α=0.05).

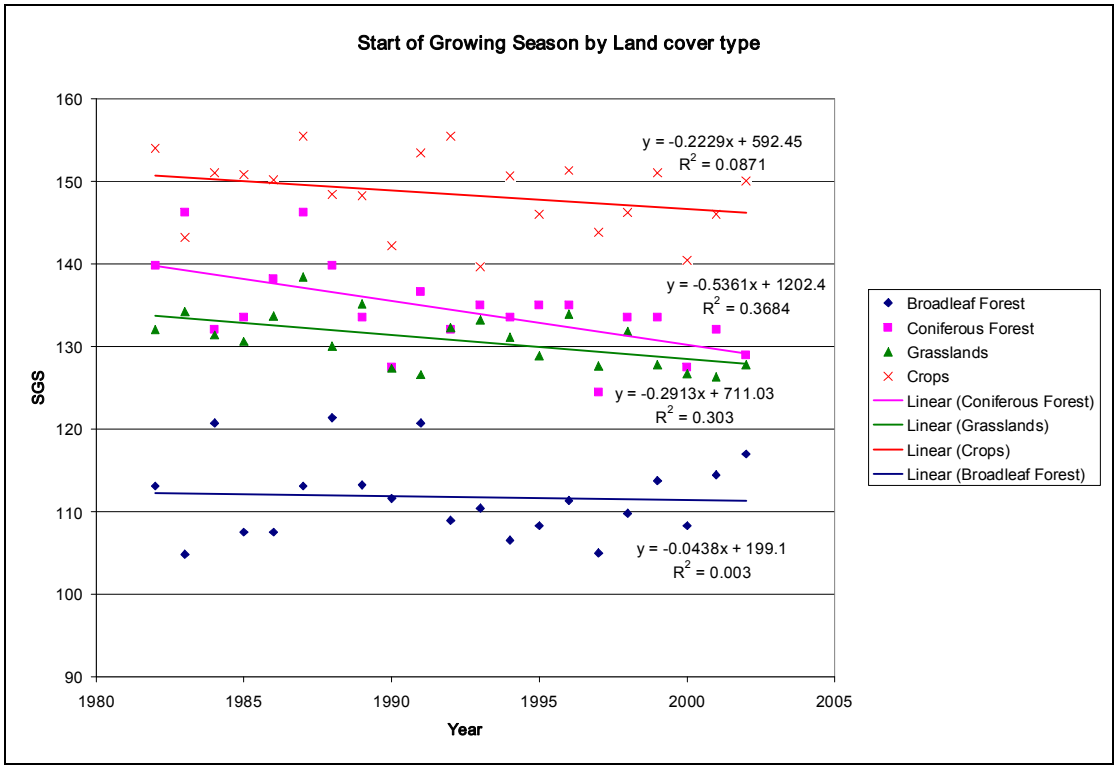

Figure 4-9. Start of Growing Season by land cover type (1982-2002)

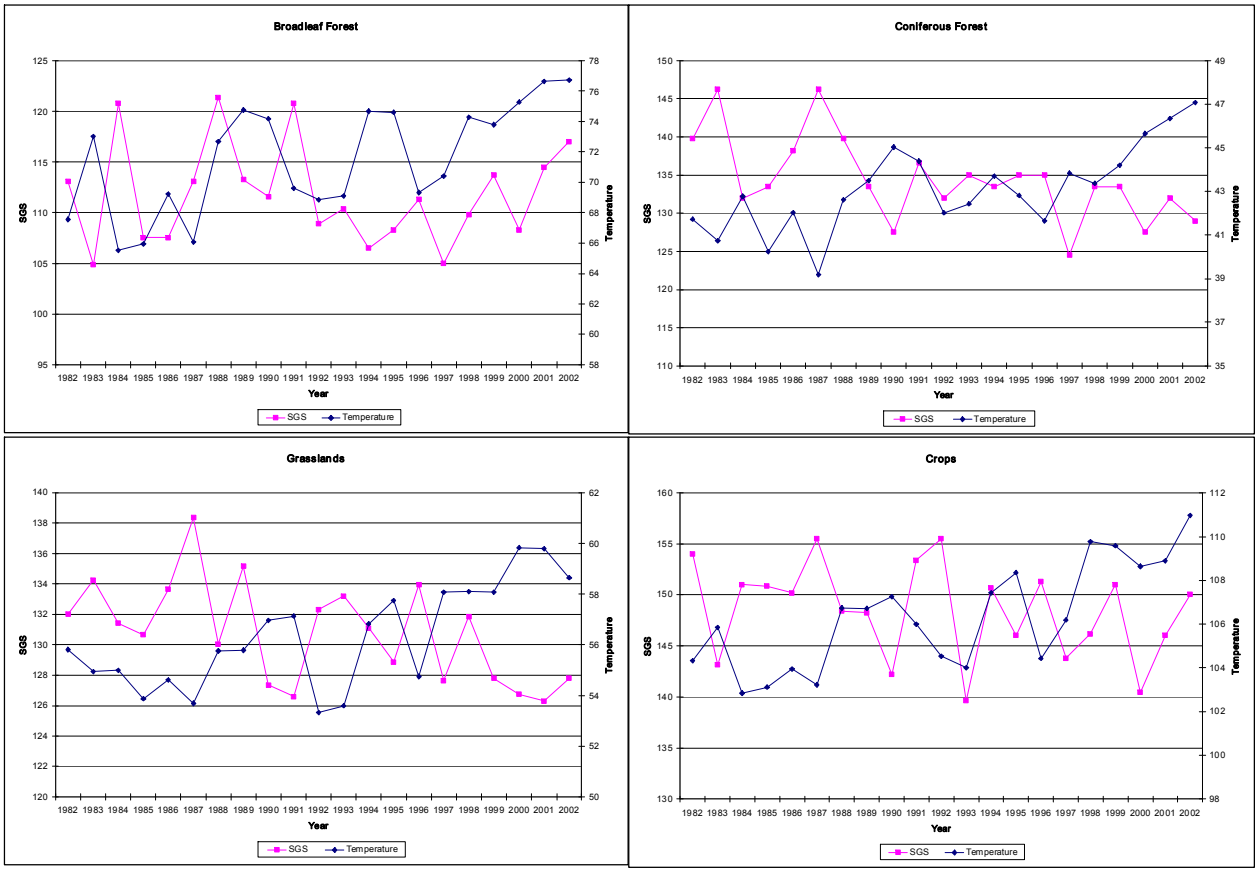

Figure 4-10. Start of Growing Season and temperature sum by land cover type (1982-2002)

Discussion

Coniferous forest and grasslands were the only two land cover types that presented statistically significant earlier spring. In figure 4-10 these two land cover classes show an opposite trend to temperature sum as expected, the higher the temperatures, the lower the SGS day.

In the case of broadleaf forest, the regression between SGS and cumulative temperature is not significant, but in figure 4-10, during almost all the years an opposite trend between these two variables is present. Broadleaf forest is the land cover class with the least pixels in this study, which may be a reason why it is difficult to detect a clear relationship between SGS and cumulative temperature.

Crops show a very low R^2 in figure 4-9, and in some years an opposite behavior of SGS with cumulative temperature. Due to the fact that crops are not a natural type of vegetation, it is not enough to relate this land cover class only to cumulative temperature, but more factors could be explaining this behavior.

4.3.2. Growing season length

In figure 4-11, the extent of the growing season shows a significant increase (α=0.05) only for coniferous forest.

GSL for broadleaf forest, grasslands and crops have a non-significant relationship with cumulative temperature (figure 4-11) and in figure 4-12 the lines of GSL and cumulative temperature behave opposed in many years.

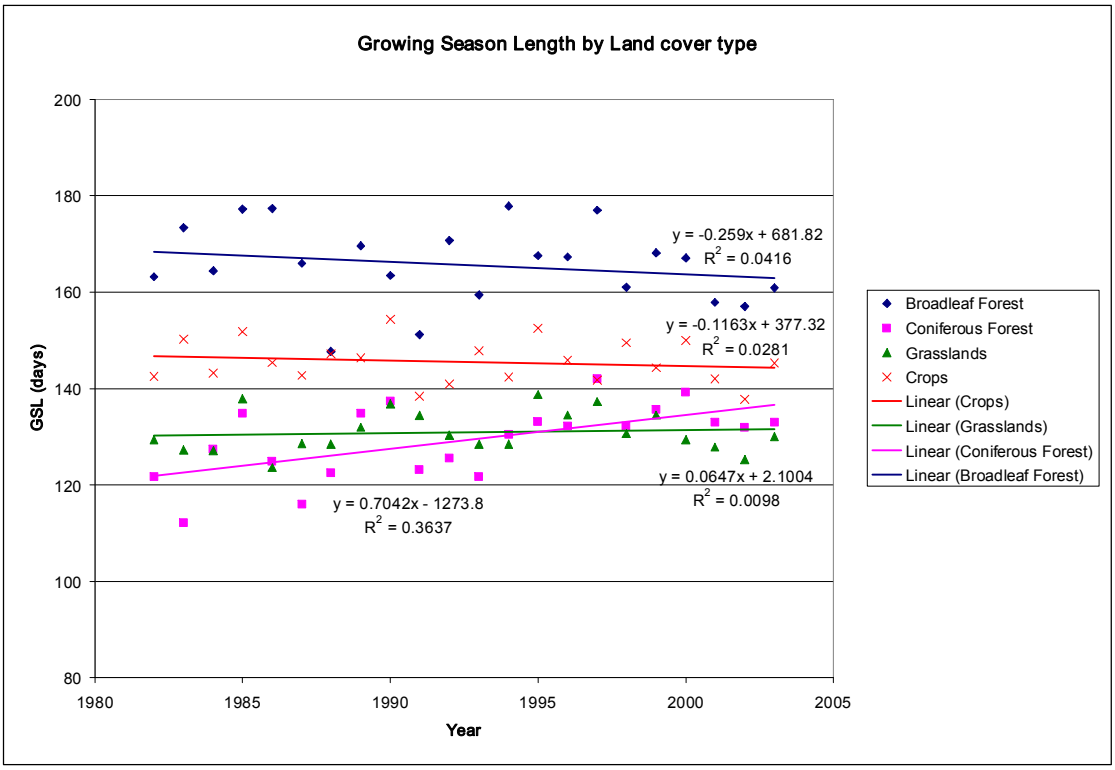

Figure 4-11. Growing Season Length by land cover type (1982-2002)

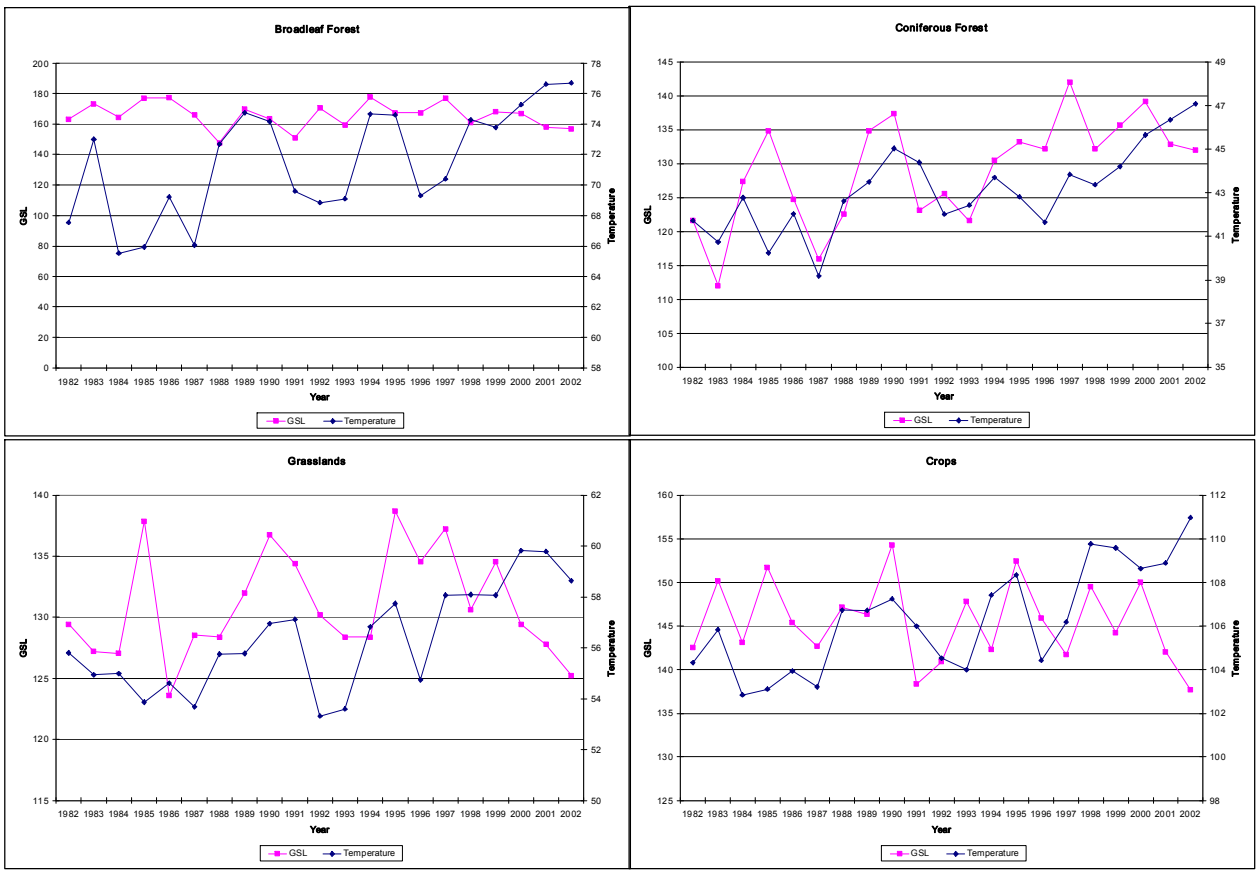

Figure 4-12. Growing Season Length and temperature sum by land cover type (1982-2002)

Discussion

White et al. (1999) concluded that there is a recent trend in colder, northern sites toward a longer GSL, but not in moderate and warm climates. Crops and grasslands have most of the pixels located in the warmest parts of Eurasia and broadleaf forest in moderate temperature areas on average. This could be the reason for GSL not behaving as with coniferous forest. Linderholm (2006) says that at lower latitudes, factors as precipitation and evapotranspiration could be playing a more important role to explain GSL than only temperature.

4.4. Regression analysis

Results of the regression of all samples taken in North and South latitudes (per land cover type) against cumulative temperature will be given. All results per sample are in the appendix, figures 8-1 to 8-12 and table 8-1.

4.4.1. Regression Phase vs. Temperature

For all land cover types, the regression of phase one vs. cumulative temperature was done per sample pixel.

In table 4-1, the R^2 showed to be significant ($\alpha = 0.05$) for the relationship between broadleaf forest phase (North sample) and cumulative temperature, with 33% of the variation in phase explained by the variation in cumulative temperature (0.33 value of R^2).

Coniferous forest (North) also showed a significant relationship with cumulative temperature, an R^2 of 0.17 is on the edge of significance for a sample size of n=21.

For crops North and South the R^2 was significant, 0.63 and 0.24, respectively.

The Pearson correlation result shows a positive and high correlation between phase and temperature sum for broadleaf forest (N), coniferous forest (N) and crops (N). Only crop (S) class shows a negative correlation, and this value is also high.

Regression	Sample	R^2	Pearson Correlation
Phase-Tcum	Broadleaf Forest (N)	0.331	0.576
	Broadleaf Forest (S)	0.042	0.205
	Coniferous Forest (N)	0.167	0.408
	Coniferous Forest (S)	0.036	-0.19
	Grasslands (N)	0.105	0.324
	Grasslands (S)	0.036	0.189
	Crops (N)	0.631	0.795
	Crops (S)	0.244	-0.494

Table 4-1. R^2 values for North and South samples by land cover types.

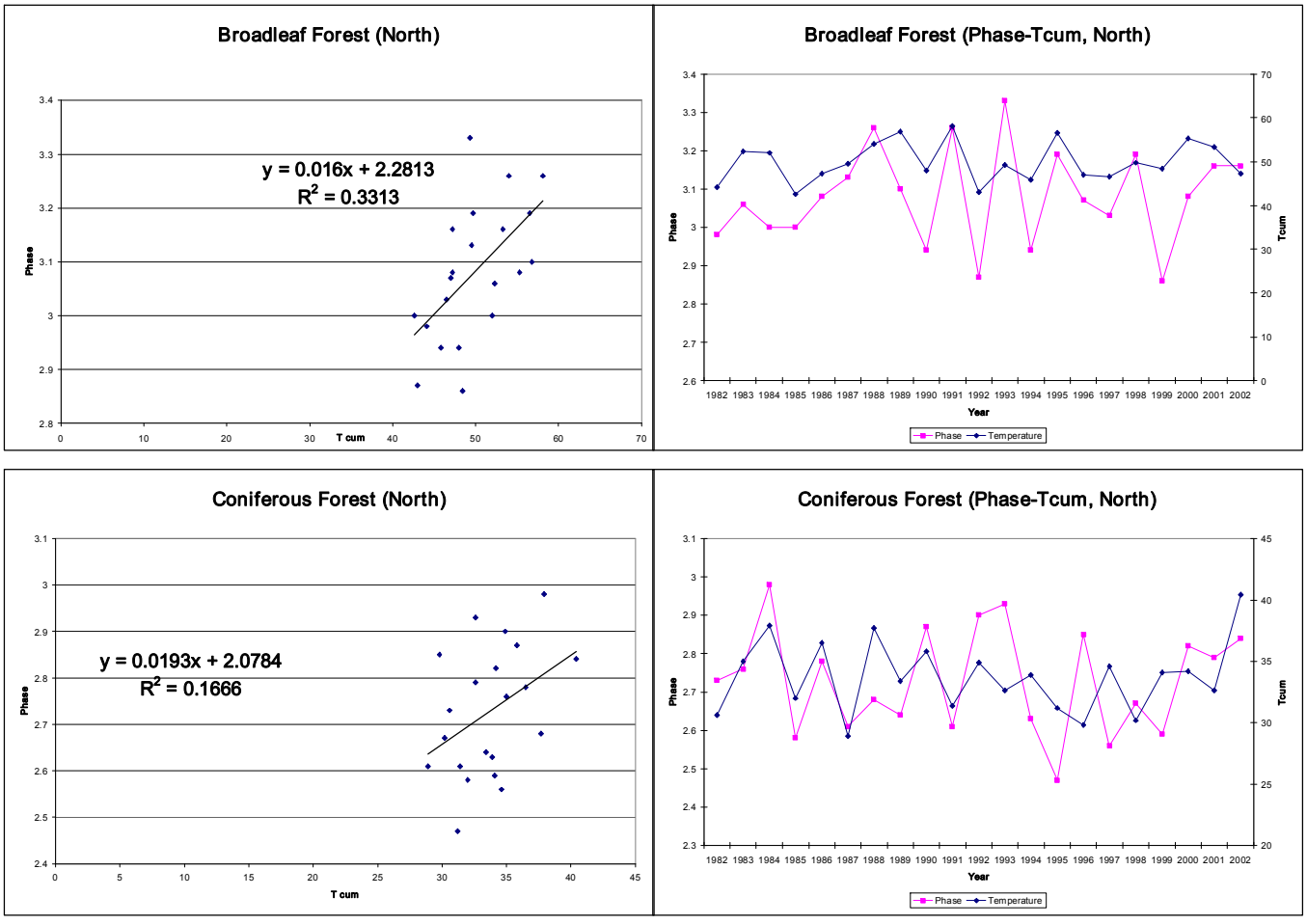

Figure 4-13. Broadleaf forest (N) and coniferous forest (N) regression and trends of phase and temperature sum

Discussion

On average the phase for north samples shows a better relationship with cumulative temperature than phase for south samples. From four land cover classes only grasslands did not show a significant relationship between phase and cumulative temperature. This result contradicts what we found in figure 4-8 where phase and temperature sum had an almost similar trend. This vegetation type is not well described; a possible reason is the small sample size.

Crops in northern parts of Eurasia show the highest R^2. The relationship between phase 1 and temperature sum is high and changes in phase can be well explained by changes in cumulative temperature. One of the most important variables that could be determining the planting of crops is temperature. At northern latitudes temperature is explaining a higher percentage of the variation in phase.

For all significant relationships, the Pearson correlation coefficient is high and positive, except between crops (S) and cumulative temperature. Figure 4-13 shows as an example two significant samples and the trend of phase and cumulative temperature through the years is quite similar.

In comparison to Zhou et al. (2001), for areas between 40˚N and 70˚N in Eurasia, the relationship between changes in NDVI and surface temperature showed to be also significant ($\alpha = 0.05$), with an R^2 of 0.752 for this part of Eurasia. The significance of their result is higher than our results for areas at that range of latitudes.

4.4.2. Regression phenological indicators vs. Temperature

After the regression analysis the table 4-2 summarizes the relationship found between the phenological indicators (SGS and GSL) and cumulative temperature.

For GSL and cumulative temperature, R^2 is significant only for coniferous forest (S) with 21% of variation of GSL explained by cumulative temperature.

The highest R^2 between SGS and temperature is found for broadleaf forest (N) and crops (N), explaining 27% and 19% of the variation, respectively.

The Pearson correlation values are given for all land cover types, taking into account the correlation between SGS, GSL and cumulative temperature.

In the case of SGS and temperature, all correlations for significant relationships are negative, broadleaf forest (N) and crops (N) are the land cover types showing higher correlation between SGS and cumulative temperature (0.52 and 0.43, respectively). Considering GSL and temperature, coniferous forest shows a negative and high correlation (0.46) between GSL and cumulative temperature.

Regression	Sample	R^2	Slope	Intercept	Pearson Correlation
GSL-Tcum	Broadleaf Forest (N)	0.103	2.253	17.407	0.32
	Broadleaf Forest (S)	0.097	-3.459	399.212	-0.311
	Coniferous Forest (N)	0.003	0.426	137.04	0.059
	Coniferous Forest (S)	0.209	-8.209	484.239	-0.457
	Grasslands (N)	0.0004	0.148	107.474	0.02
	Grasslands (S)	0.139	-7.02	1558.852	-0.373
	Crops (N)	0.067	-1.635	279.773	-0.258
	Crops (S)	0.064	-3.007	694.064	-0.252
SGS-Tcum	Broadleaf Forest (N)	0.268	-2.329	240.595	-0.518
	Broadleaf Forest (S)	0.066	1.175	41.61	0.258
	Coniferous Forest (N)	0.004	-0.592	145.13	-0.07
	Coniferous Forest (S)	0.079	6.042	-59.275	0.282
	Grasslands (N)	0.119	-1.443	164.659	-0.344
	Grasslands (S)	0.132	-14.519	3139.42	-0.363
	Crops (N)	0.187	-0.855	154.208	-0.433
	Crops (S)	0.032	3.446	-419.005	0.181

Table 4-2. R^2 values for SGS and GSL for all land cover types

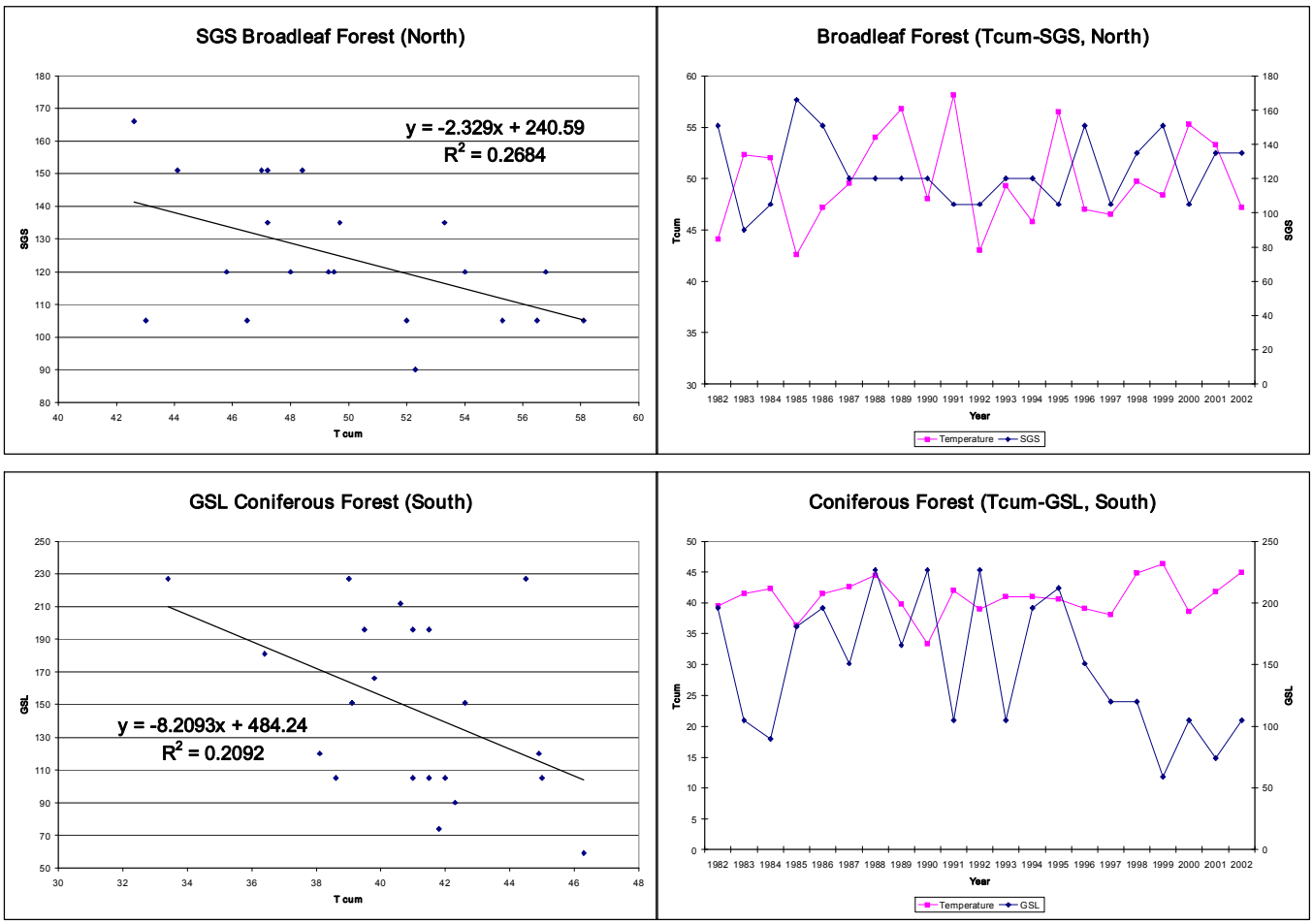

Figure 4-14. SGS and GSL for two significant relationships with cumulative temperature

Discussion

SGS and GSL showed fewer samples that were statistically significant than phase. For SGS, only two land cover types located at the northern latitudes showed a significant relationship with cumulative temperature. GSL presents only one statistically significant relationship for the south sample of coniferous forest.

Analyzing Pearson coefficients for the significant relationships, SGS and cumulative temperature present negative coefficients indicating higher temperatures leading to lower SGS, or an earlier growing season is expected as result of higher temperatures. Figure 4-14 shows an opposite trend between SGS of broadleaf forest (N) and cumulative temperature lines as expected.

GSL and cumulative temperature for coniferous forest, although appearing with a significant relationship, also shows an opposite trend between the two variables. Pearson coefficient is negative for this sample, meaning at high temperatures shorter GSL. Vedin (1990) found that GSL and temperature are not necessarily correlated as expected, and warm growing seasons do not mean they will be automatically longer. Jones et al. (2002) concluded that GSL is better correlated to annual temperatures than to seasonal ones; in our case cumulative temperature is seasonal and this could be the reason of finding poor correlations.

5. CONCLUSIONS

This study has shown an ascending trend for the yearly sum of temperatures from January to July (1982-2002) for the area of Eurasia where the four land cover classes (broadleaf and coniferous forests, grasslands and crops) under study are located.

The land cover class crops is located in areas with the highest temperature sum, with a large amount of pixels located at latitudes under 40° N. Broadleaf forest, grasslands and coniferous forest have a descending order of temperature sum for the areas where they grow. This result is consistent with the types of vegetation and the adaptation they show to temperature. For instance, coniferous forest is composed by types of trees which are able to grow under freezing temperatures.

HANTS results of amplitude for the first and second harmonics were useful to detect, by means of the ratio of amplitudes, if vegetation shows a one or half yearly cycle. The one yearly cycle behavior of vegetation was predominant for all land cover classes. In the case of some areas of crops in China and Bangladesh, a change of one to half yearly cycle became predominant, showing that crops are being cultivated more than once a year in those areas towards the end of the 21-year period studied.

HANTS results of phase could indicate changes in temperature sum for some land cover classes. From the averaged (by land cover type) phase results of HANTS, we conclude that phase and temperature sum behave in the same way for most of the analyzed years. Plotting the phase 1 against temperature sum showed for most of the land cover types that the trend of both curves was similar (same peeks and valleys) for almost all the years analyzed. In the case of Coniferous Forest, this trend was not as clear as it was for the other three land cover types.

From the regression analysis between phase and temperature sum for the sample pixels (in north and south pixels), northern samples for broadleaf forest, coniferous forest and crops showed a significant correlation (α=0.05). Crop land cover type was the only land cover type with a south significant sample pixel. Grasslands land cover

type showed no significant relationship at all (neither north nor south pixels) with temperature sum. A small sample size leads to a contradiction between the averaged pixels and the sample pixels for that land cover type.

Studying the trends of SGS (averaged pixels per land cover type) and temperature sum, just coniferous forest and grasslands showed a significant relationship (α=0.05) that helps us to conclude that the growing season, in the case of these land cover types, is starting earlier while the temperatures are increasing. Studying the relationship of SGS and temperature sum for sample pixels at north and south latitudes, broadleaf forest and crops (for northern pixels) were the only two land cover classes which showed significant relationships (α=0.05). In this case, the small sample could be playing an important role to find this contradictory result. From the significant sample pixels, only northern ones were the best to observe relationships between SGS and temperature sum due to the importance that temperature has over other climatic factors for plant growth at high latitudes.

For GSL (averaged pixels per land cover type) and temperature sum, the regression showed significance (α=0.05) only for coniferous forest. For the sample pixels, coniferous forest (pixel in the south) was also the only land cover class which showed a significant relationship (α=0.05) between GSL and temperature sum. The small sample size is affecting the results and also the fact that seasonal temperatures instead of annual temperatures are being used.

As a general conclusion, HANTS outputs were useful to detect seasonality of the land cover classes under study, by means of the ratio of amplitudes. The phenologic changes that are being observed as a result of global warming were also found for some land cover types using this methodology. Analyzing the relationship between phase and temperature sum we could find more significant relationships than using the phenological indicators and temperature sum. Phase could be a good indicator of temperature as a driver of changes in vegetation. However, further research could help to understand these results.

6. RECOMMENDATIONS

Some drawbacks were encountered while carrying out this work and some improvements could be made in order to achieve better results and get more information. One of the main improvements would be to perform a spatial regression analysis (pixel by pixel). An stratification according to latitude and a regression analysis performed by stratum should give better results. In this way the problems while averaging zones with extreme values of temperature or other variables because of geographic location would be avoided. For instance pixels at north latitudes do not show temperatures as high as pixels located in southern areas. Time constrain did not let us do this type of analysis.

Other climatic variables could be used in order to observe which climate variables are affecting phenology at the different latitudes.

GSL should be analyzed using annual temperatures instead of seasonal ones, because this phenological indicator covers yearly periods.

7. REFERENCES

Askeyev, O., Tischin, D., Sparks, T., Askeyev, I. 2005. The effect of climate on the phenology, acorn crop and radial increment of pedunculate oak (Quercus robur) in the middle Volga region, Tatarstan, Russia. Int J Biometeorol, 49:262–266 DOI 10.1007/s00484-004-0233-3

Azzali, S. and Menenti, M. 2000. Mapping vegetation-soil-climate complexes in southern Africa using temporal Fourier analysis of NOAA-AVHRR NDVI data. International Journal of Remote Sensing, Vol. 21, No. 5, 973-996.

Bogaert, J., Zhou, L., Tucker, C., Myneni, R. and Ceulemans, R. 2002. Evidence for a persistent and extensive greening trend in Eurasia inferred from satellite vegetation index data. Journal of Geophysical Research, Vol. 107, No. D11

Botta, A., Viovy, N., Ciais, P., Friedlingstein, P. and P. Monfray. 2000. A global prognostic scheme of leaf onset using satellite data. Global Change Biology, 6, 709-725.

Chen, X., Tan, Z., Schwartz, M. and Xin, C. 2000. Determining the growing season of land vegetation on the basis of plant phenology and satellite data in Northern China. International Journal of Biometeorology, Vol. 44, 97-101

De Wit, A. and Su, B. 2004. Deriving phenological indicators from SPOT-VGT data using the HANTS algorithm. Center for Geo-information, Wageningen-UR.

Dose, V., Menzel, A. 2004. Bayesian analysis of climate change impacts in Phenology. Global Change Biology, 10, 259–272

EPN. 2006. URL: http://www.dow.wau.nl/msa/gpm/. 08/02/2006

Feddema, J., Oleson, K., Bonan, G., Mearns, L., Buja, L., Meehl, G. and Washington, W. 2005. The Importance of Land-Cover change in simulating future climates. Science, Vol. 310, 1674-1678.

Fisher, J., Mustard, J. and Vadeboncoeur, M. 2006. Green leaf phenology at Landsat resolution: Scaling from the field to the satellite. Remote Sensing of Environment, 100, 265-279.

GIMMS, 2005. Documentation of 2003.
URL:
http://ltpwww.gsfc.nasa.gov/gimms/htdocs/ndvi/ndvie/GIMMSdocumentation_NDVIe.pdf

Immerzeel, W., Quiroz, R. and De Jong, S. 2005. Understanding precipitation patterns and land use interaction in Tibet using harmonic analysis of SPOT VGT-S10 NDVI time series. International Journal of Remote Sensing, Vol. 26, No. 11, 2281-2296.

Intergovernmental Panel of Climate Change (IPCC). 2001. Climate Change 2001:The Scientific Basis.
URL: http://www.grida.no/climate/ipcc_tar/wg1/index.htm

Islam, S., Jahin Hasan, G. and Chowdhury, A. 2005. Destroying hills in the northeastern part of Bangladesh: A qualitative assessment of extent of the problem and its probable impact. Int. J. Environ. Sci. Tech., Vol. 2, No. 4, pp. 301-308

Keeling, C., Whorf, T., Wahlen, M. and van der Plicht, J. 1995. Interannual extremes in the rate of rise of atmospheric carbon dioxide since 1980. Nature, Vol. 375, 666-670

Koulakov, I. 1998. Three-dimensional seismic structure of the upper mantle beneath the central part of the Eurasian continent. Geophys. J. Int., 133, 467-489.

Kross, A. 2005. Evaluating the applicability of MODIS data for Phenological Monitoring in The Netherlands. Thesis Report for Centre for Geo-Information, Wageningen University.

Lillesand, T., Kiefer, R. and Chipman, J. 2004. Remote Sensing and Image Interpretation. John Wiley & Sons Inc.

Linderholm, H. 2006. Growing Season changes in the last century. Agricultural and Forest Meteorology, 137, 1-14.

Masson, V., Champeaux, J., Chauvin, F., Meriguet, C. and Lacaze, R. 2003. A Global Database of Land Surface Parameters at 1-km Resolution in Meteorological and Climate Models. Journal of Climate, Vol. 16, No. 9, 1261-1281.

Menzel, A. 2003. Plant phenological anomalies in Germany and their relation to air temperature and NAO. Climatic Change, 57, 243–263.

Menzel, A. 2000. Trends in phenological phases in Europe between 1951 and 1996. Int J Biometeorol, 44, 76–81

Menzel, A., Fabian, P. 1999. Growing season extended in Europe. Nature, Vol. 397, www.nature.com

Moody, A. and Johnson, D. 2001. Land-surface phenologies from AVHRR using the discrete fourier transform. Remote Sensing of Environment, 75, 305-323.

Mücher, C., Roerink, G. and Metzger, M. 2002. Study of vegetation dynamics in relation to climate parameters. International workshop of The European Phenology Network – Use of Earth Observation Data for Phenological Monitoring, Proceedings. Joint Research Centre, Ispra (VA) Italy 12th and 13th December 2002

Myneni, R., Keeling, C., Tucker, C., Asrar, G. and Nemani, R. 1997. Increased plant growth in the northern high latitudes from 1981 to 1991. Nature, Vol. 386, 698-702

Nemani, R., Keeling, C., Hashimoto, H., Jolly, W., Piper, S., Tucker, C., Myneni, R. and Running, S. 2003. Science, Vol. 300, www.sciencemag.org

New, M., Hulme, M. and Jones, P. 1999. Representing Twentieth-Century Space–Time Climate Variability. Part I: Development of a 1961–90 Mean Monthly Terrestrial Climatology. Climatic Research Unit, School of Environmental Sciences, University of East Anglia, Norwich, United Kingdom. 829-856

Prasad, V., Badarinath, K., Tsuruta, H., Sudo, S., Yonemura, S., Cardina, J., Stinner, B., Moore, R., Stinner, D. and Hoy, C. 2003. Implications of Land Use Changes on Carbon Dynamics and Sequestration from Forestry Datasets, India. The Environmentalist, 23, 175-187.

Roerink, G., Menenti, M. and Verhoef, W. 2000. Reconstructing cloudfree NDVI composites using Fourier analysis of time series. International Journal of Remote Sensing, Vol. 21, No. 9, 1911-1917.

Sakamoto, T., Yokozawa, M., Toritani, H., Shibayama, M., Ishitsuka, N. and Ohno, H. 2005. A crop phenology detection method using time-series MODIS data. Remote Sensing of Environment, 96, 366 – 374.

Schwartz, M. and Reiter, B. 2000. Changes in North American spring. International Journal of Climatology, 20, 929-932.

Shabanov, N., Zhou, L., Knyazikhin, Y., Myneni, R. and Tucker, C. 2002. Analysis of Interannual Changes in Northern Vegetation Activity Observed in AVHRR Data From 1981 to 1994. IEEE Transactions on Geoscience and Remote Sensing, Vol. 40, No. 1.

Stott, P. A., Tett, S. F. B., Jones, G. S., Allen, M. R., Mitchell, J. F. B., and Jenkins, G. J. 2000. External control of twentieth century temperature variations by natural and anthropogenic forcings. Science, 15, 2133–2137.

Sutton, R. and Hodson, D. 2005. Atlantic Ocean Forcing of North American and European Summer Climate. Science, 309, 115-118

Tucker, C., Slayback, D., Pinzon, J., Los, S., Myneni, R. and Taylor, M. 2001. Higher Northern Latitude NDVI and Growing Season Trends from 1982 to 1999. http://cybele.bu.edu/download/manuscripts/tucker01.pdf

White, M., Running, S. and Thornton, P. 1999. The impact of growing-season length variability on carbon assimilation and evapotranspiration over 88 years in the eastern US deciduous forest. International Journal of Biometeorology, 42, 139-145.

Xiao, J. and Moody, A. 2005. Geographical distribution of global greening trends and their climatic correlates: 1982-1998. International Journal of Remote Sensing, Vol. 26, No. 11, 2371-2390.

Xiao, X., Boles, S., Frolking, S., Salas, W., Moore III, B. and Li, C. 2002. Observation of flooding and rice transplanting of paddy rice fields at the site to landscape scales in China using VEGETATION sensor data. International Journal of Remote Sensing, Vol. 23, No. 15, 3009-3022.

Zhang, Q., Yang, H., Zhong, Y. and Wang, D. 2005. An idealized study of the impact of extratropical climate change on El Nino-Southern Oscillation. Climate Dynamics, 25, 869-880.

Zhou, L., Tucker, C., Kaufmann, R., Slayback, D., Shabanov, N. and Myneni, R. 2001. Variations in northern vegetation activity inferred from satellite data of vegetation index during 1981 to 1999. Journal of Geophysical Research, Vol. 106, No. D17, 20069-20083.

8. APPENDIX

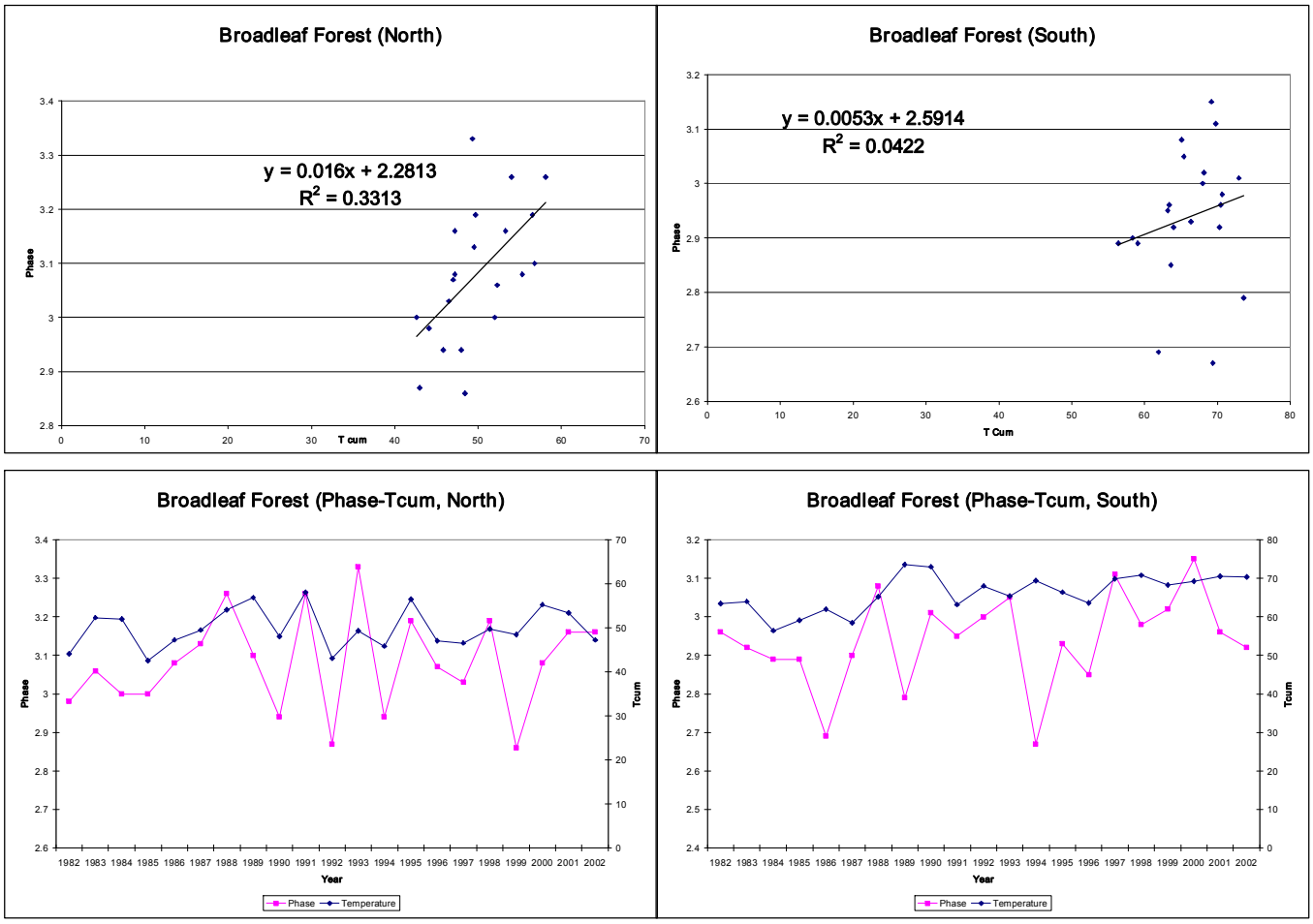

Figure 8-1. Broadleaf Forest Phase vs. Cumulative Temperature for North and South points.

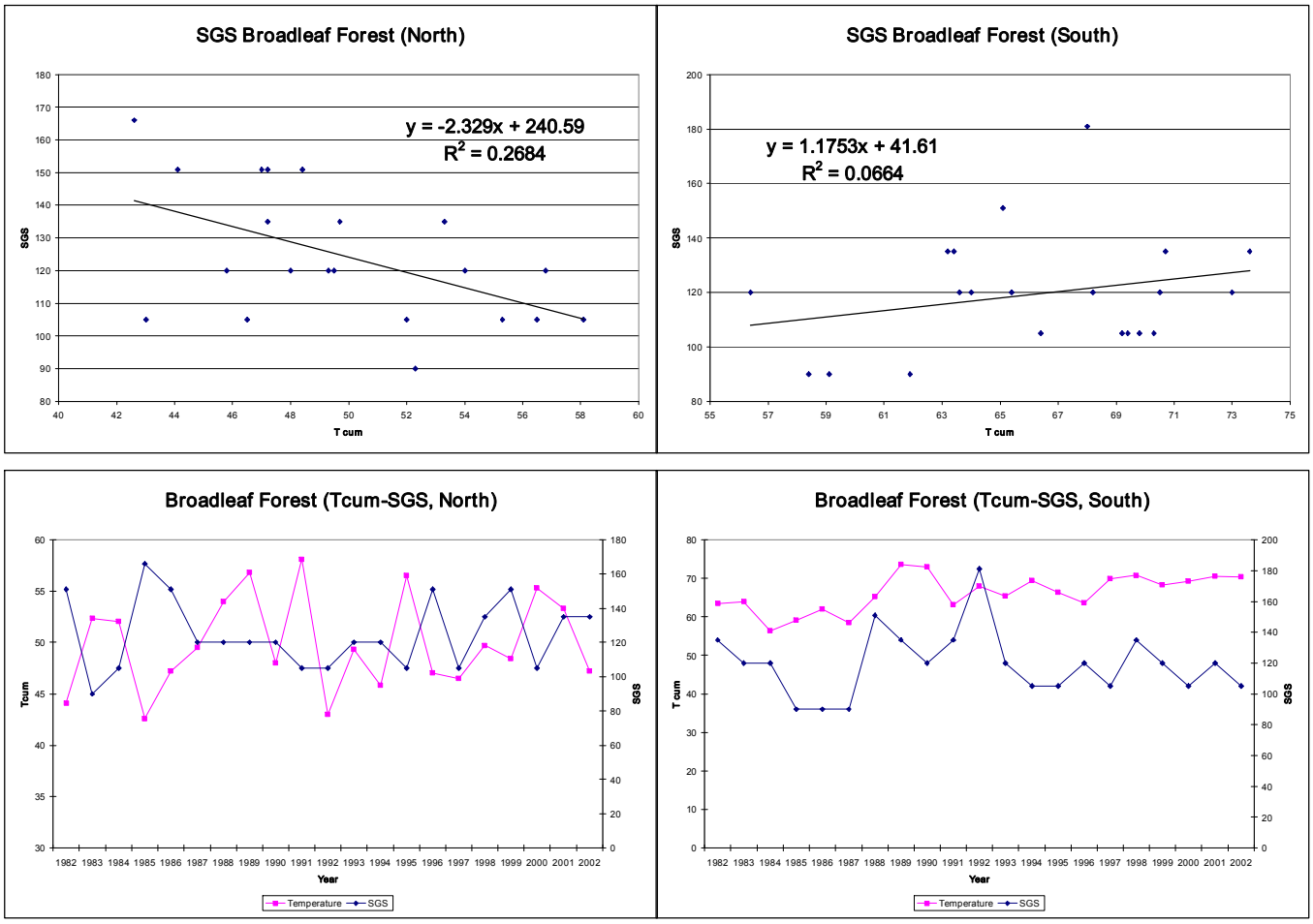

Figure 8-2. Broadleaf Forest SGS vs. Cumulative Temperature for North and South points.

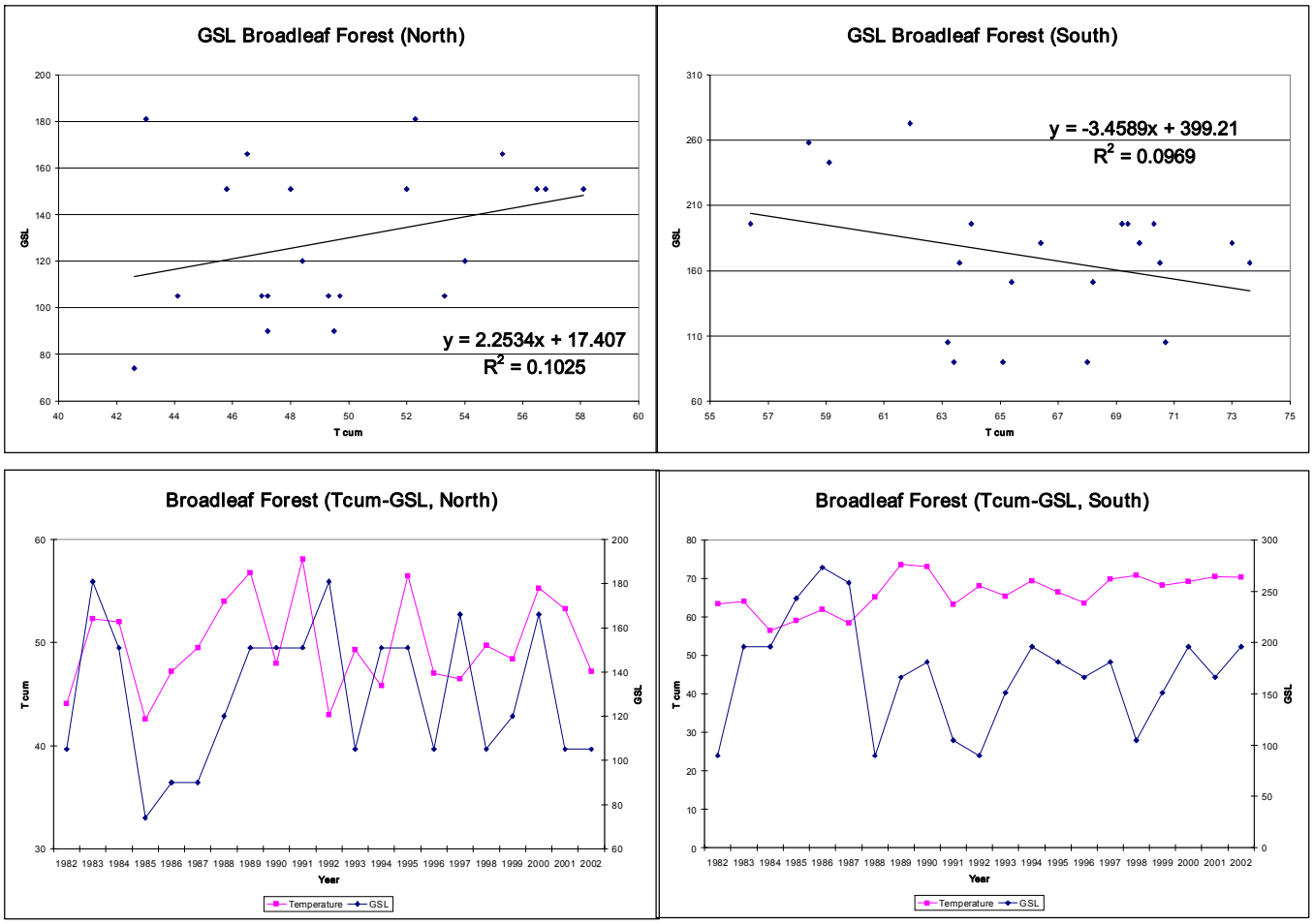

Figure 8-3. Broadleaf Forest GSL vs. Cumulative Temperature for North and South points.

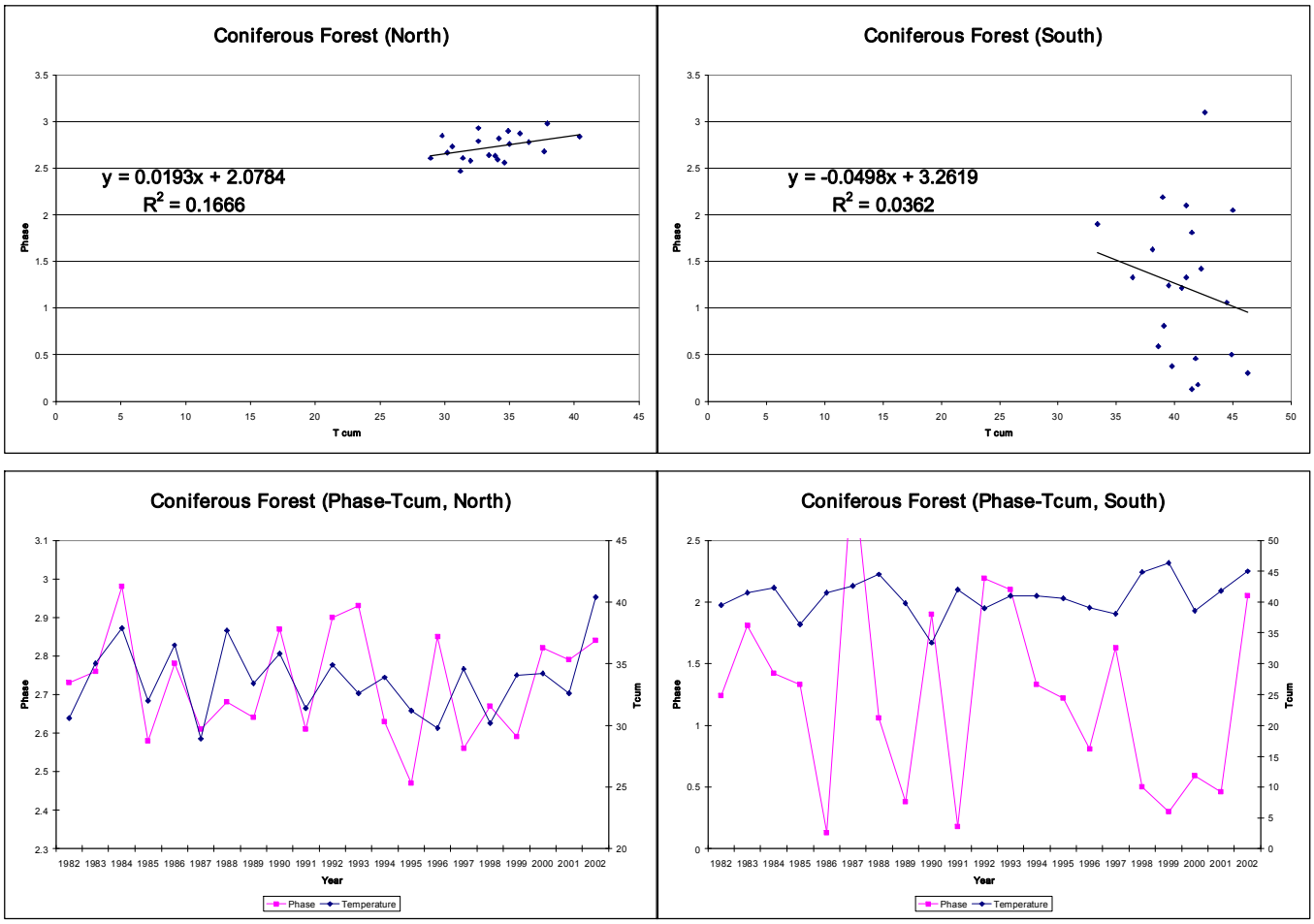

Figure 8-4. Coniferous Forest Phase vs. Cumulative Temperature for North and South points.

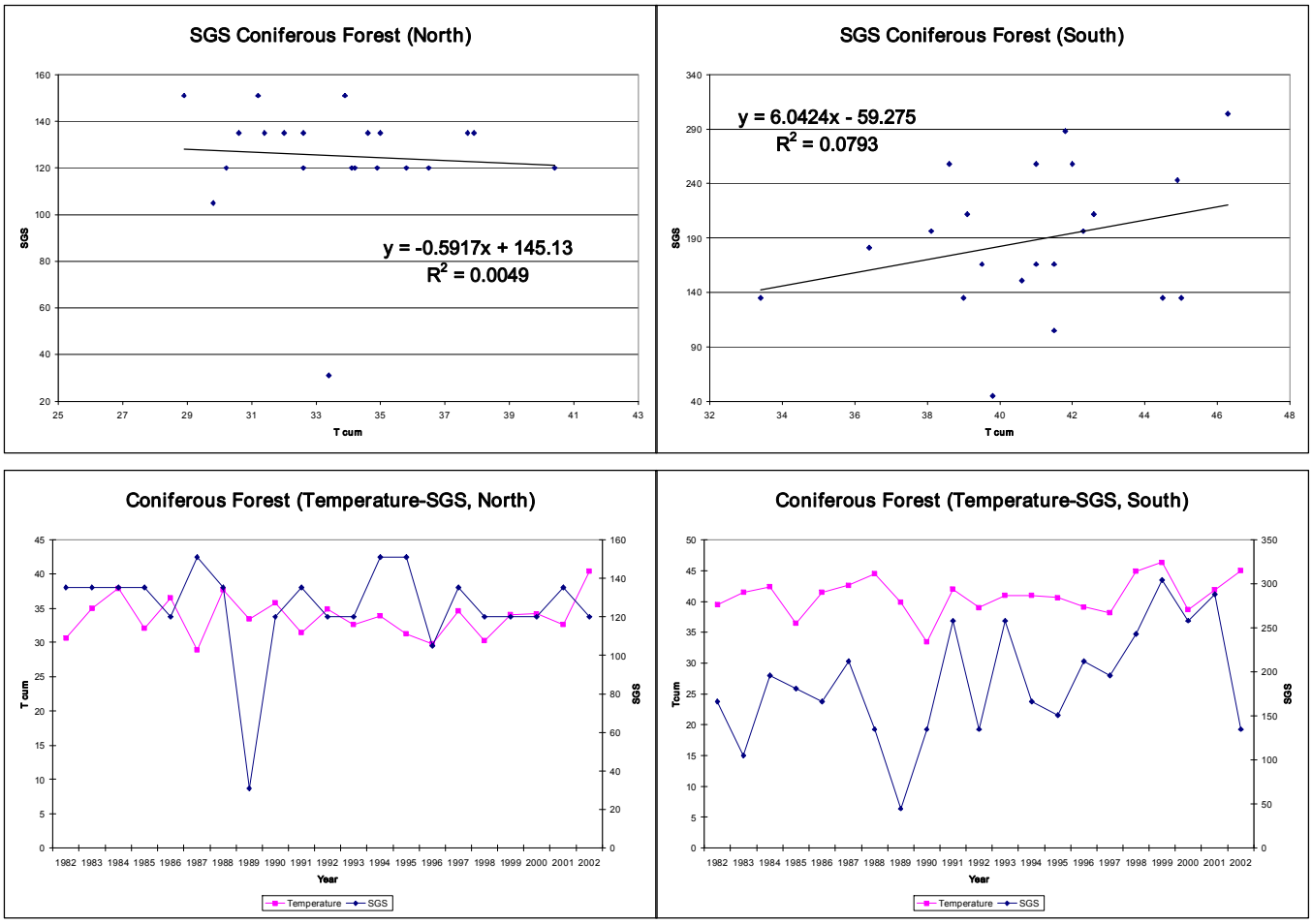

Figure 8-5. Coniferous Forest SGS vs. Cumulative Temperature for North and South points.

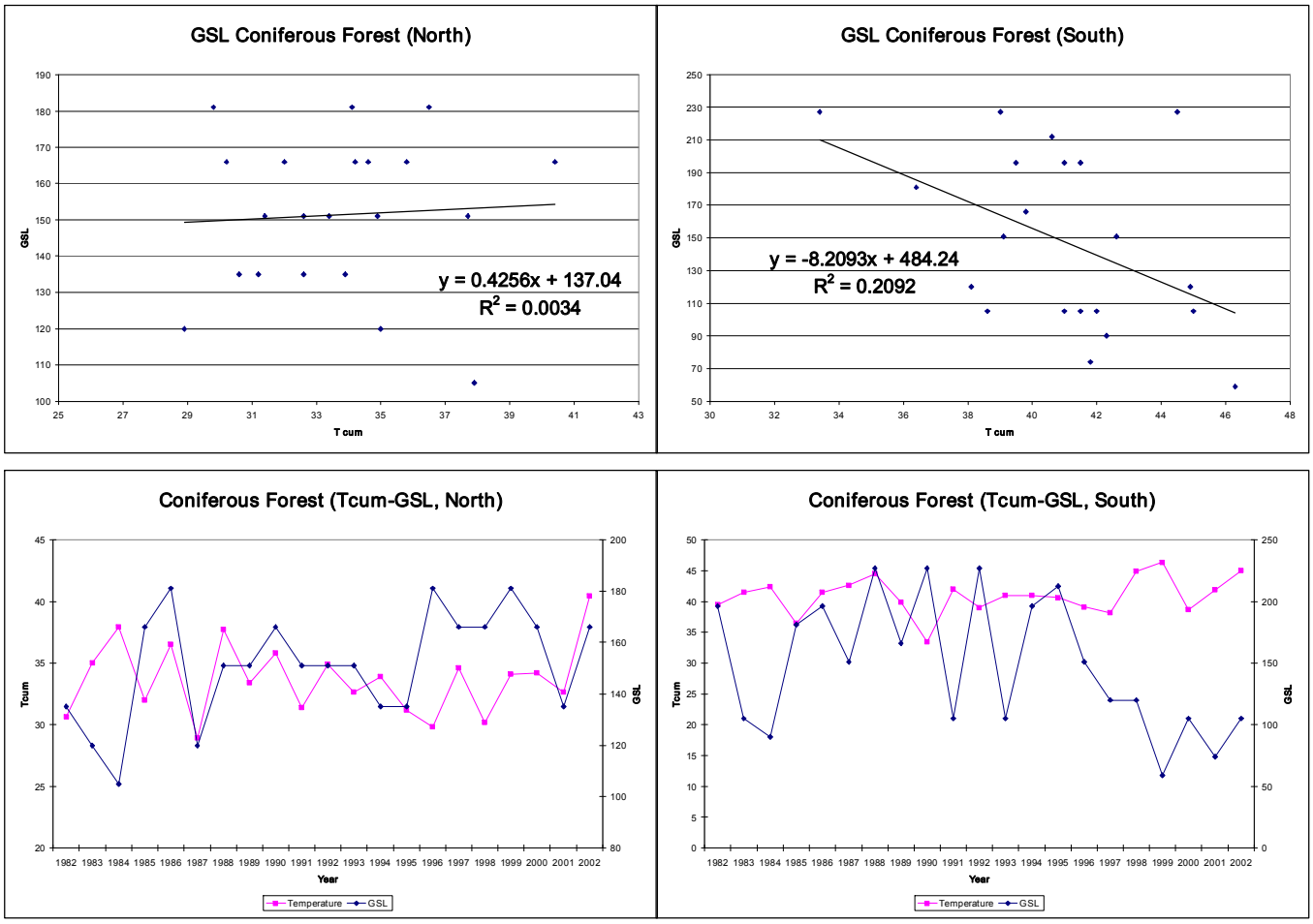

Figure 8-6. Coniferous Forest GSL vs. Cumulative Temperature for North and South points.

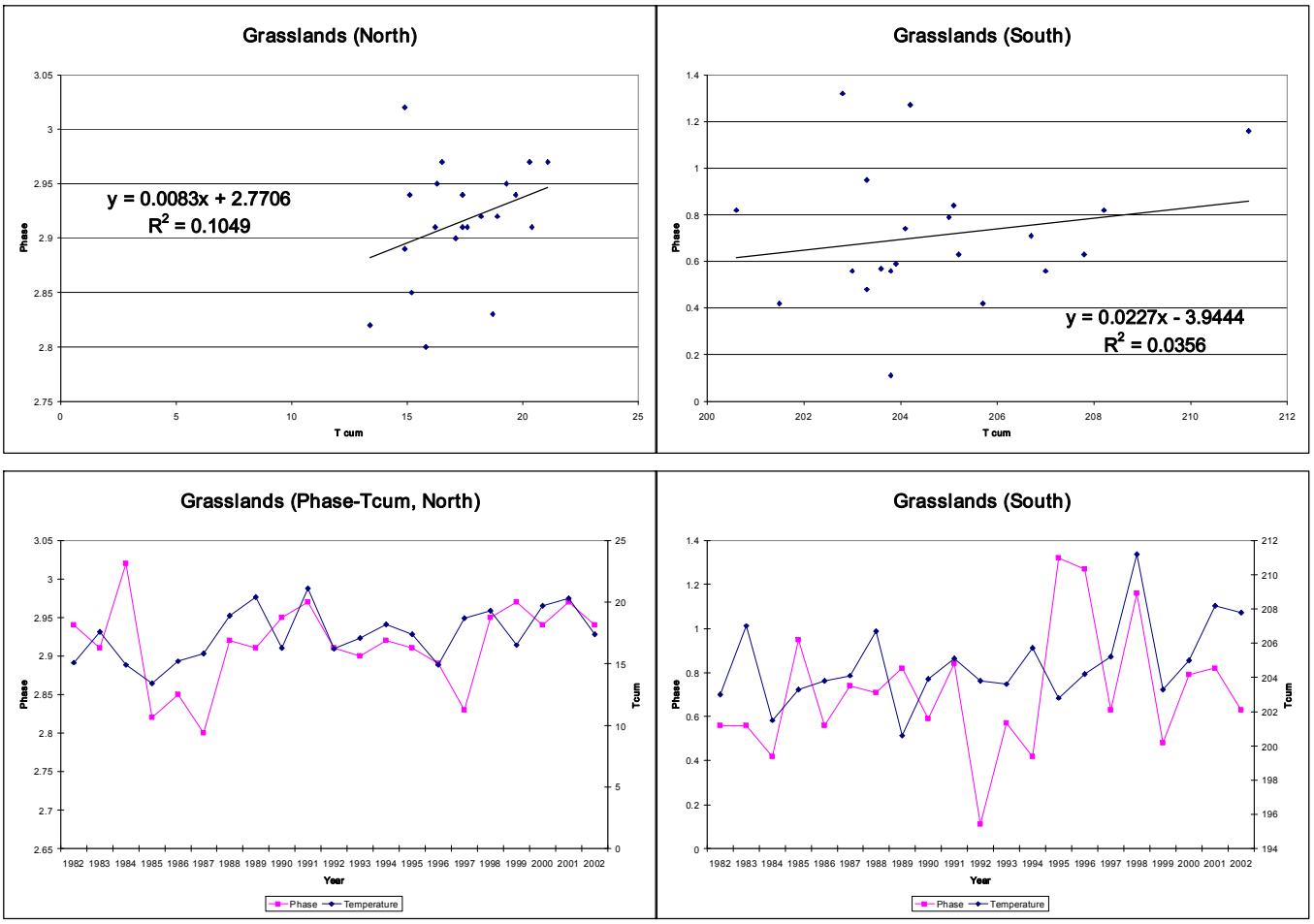

Figure 8-7. Grasslands Phase vs. Cumulative Temperature for North and South points.

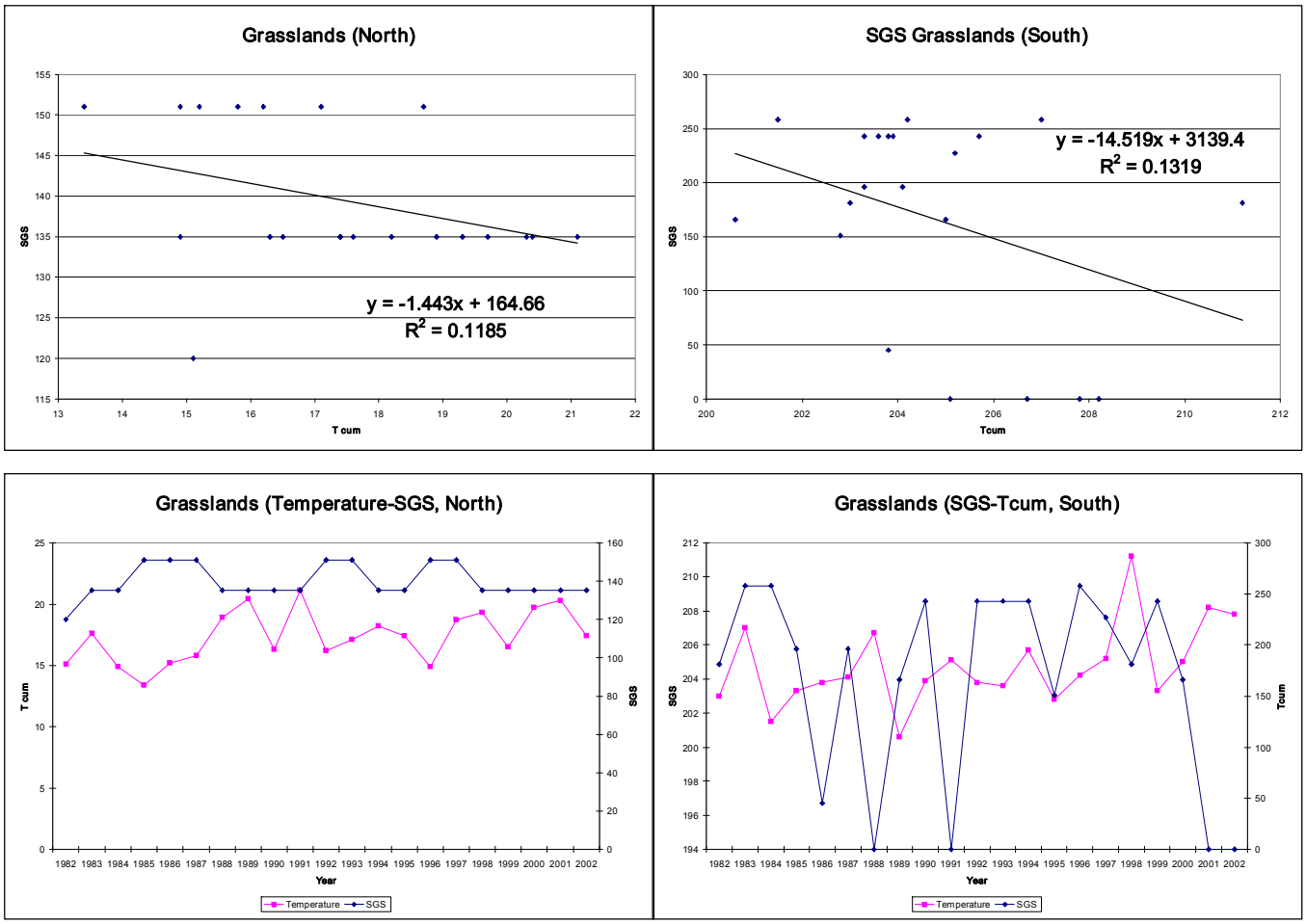

Figure 8-8. Grasslands SGS vs. Cumulative Temperature for North and South points.

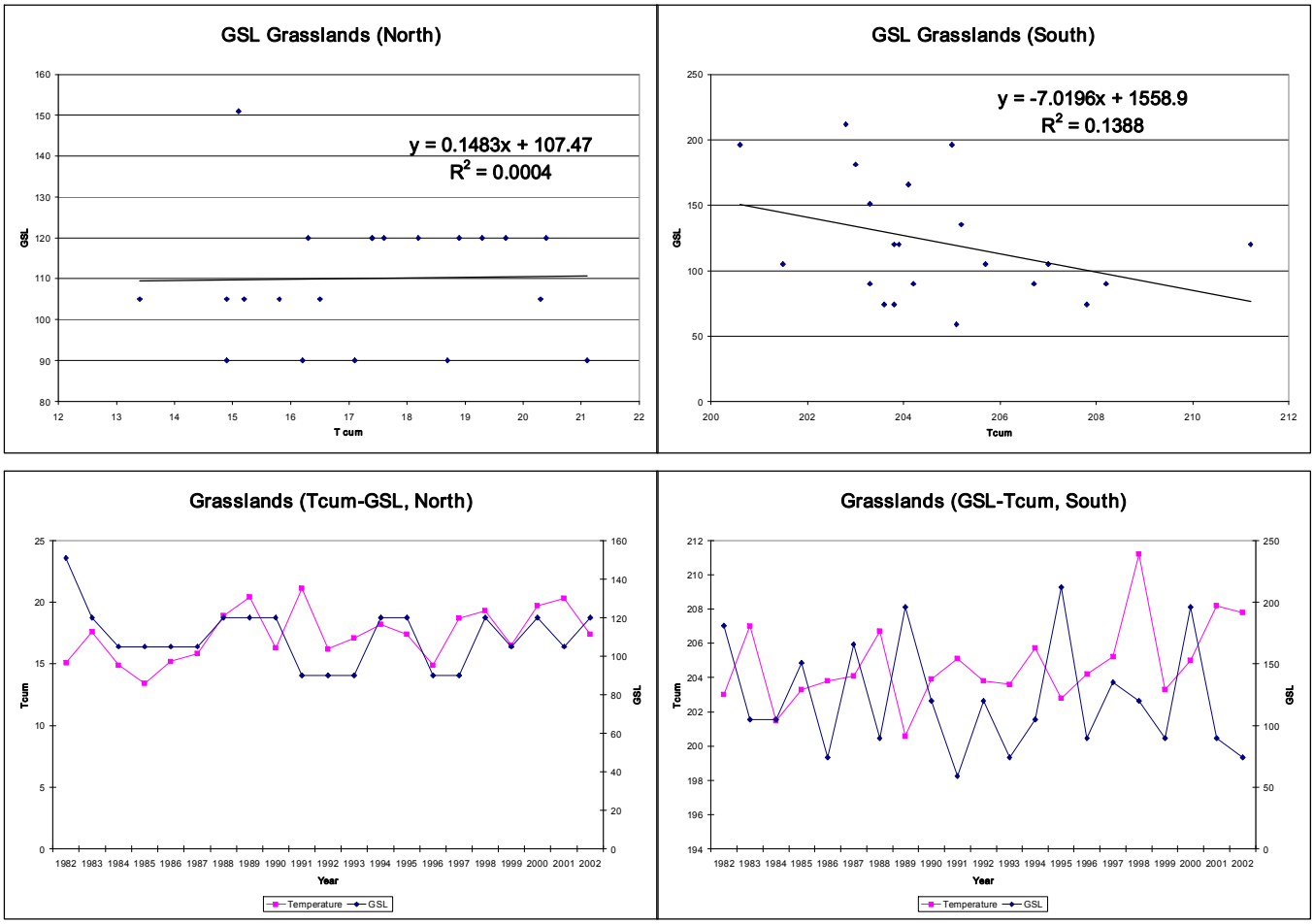

Figure 8-9. Grasslands GSL vs. Cumulative Temperature for North and South points.

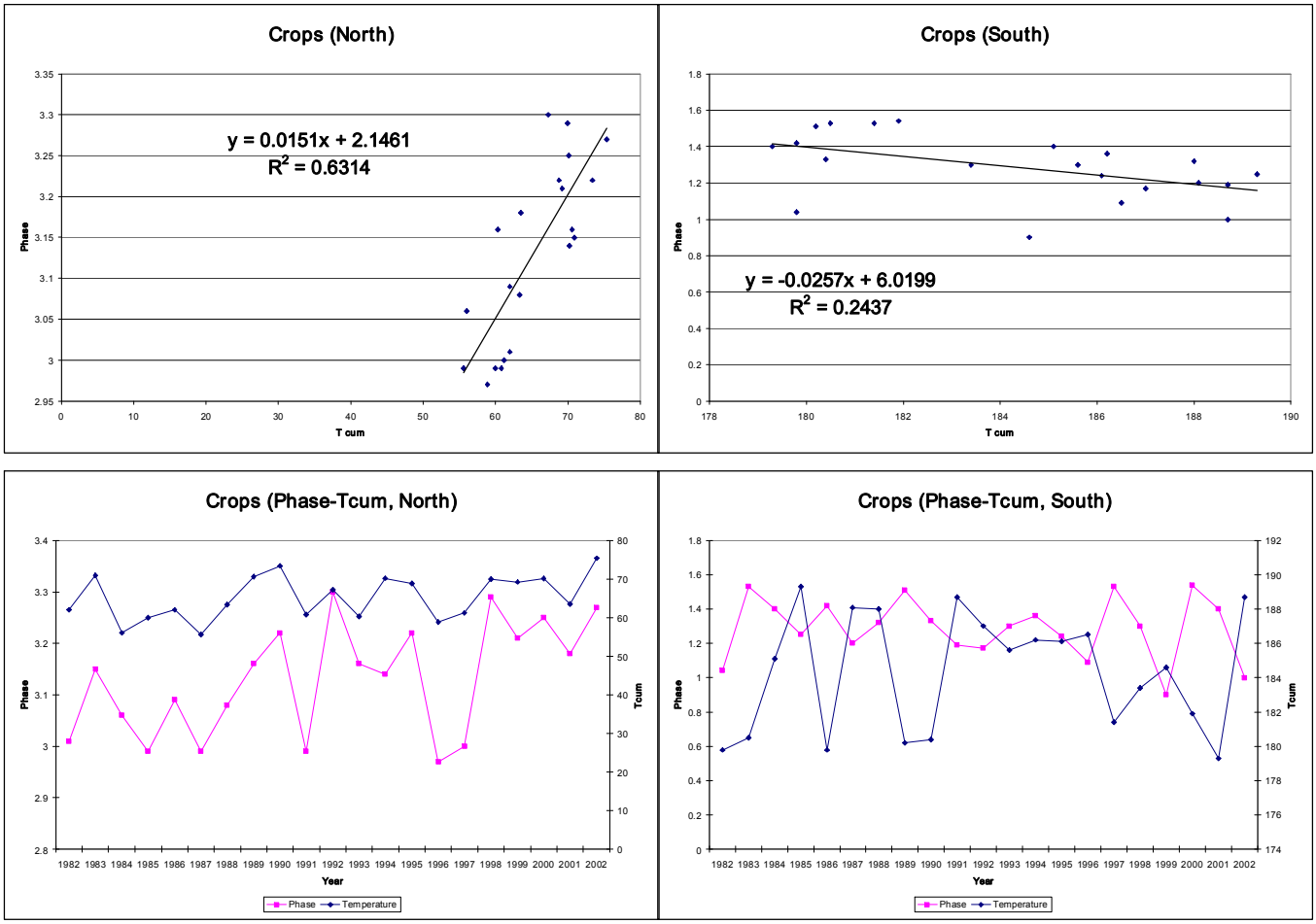

Figure 8-10. Crops Phase vs. Cumulative Temperature for North and South points.

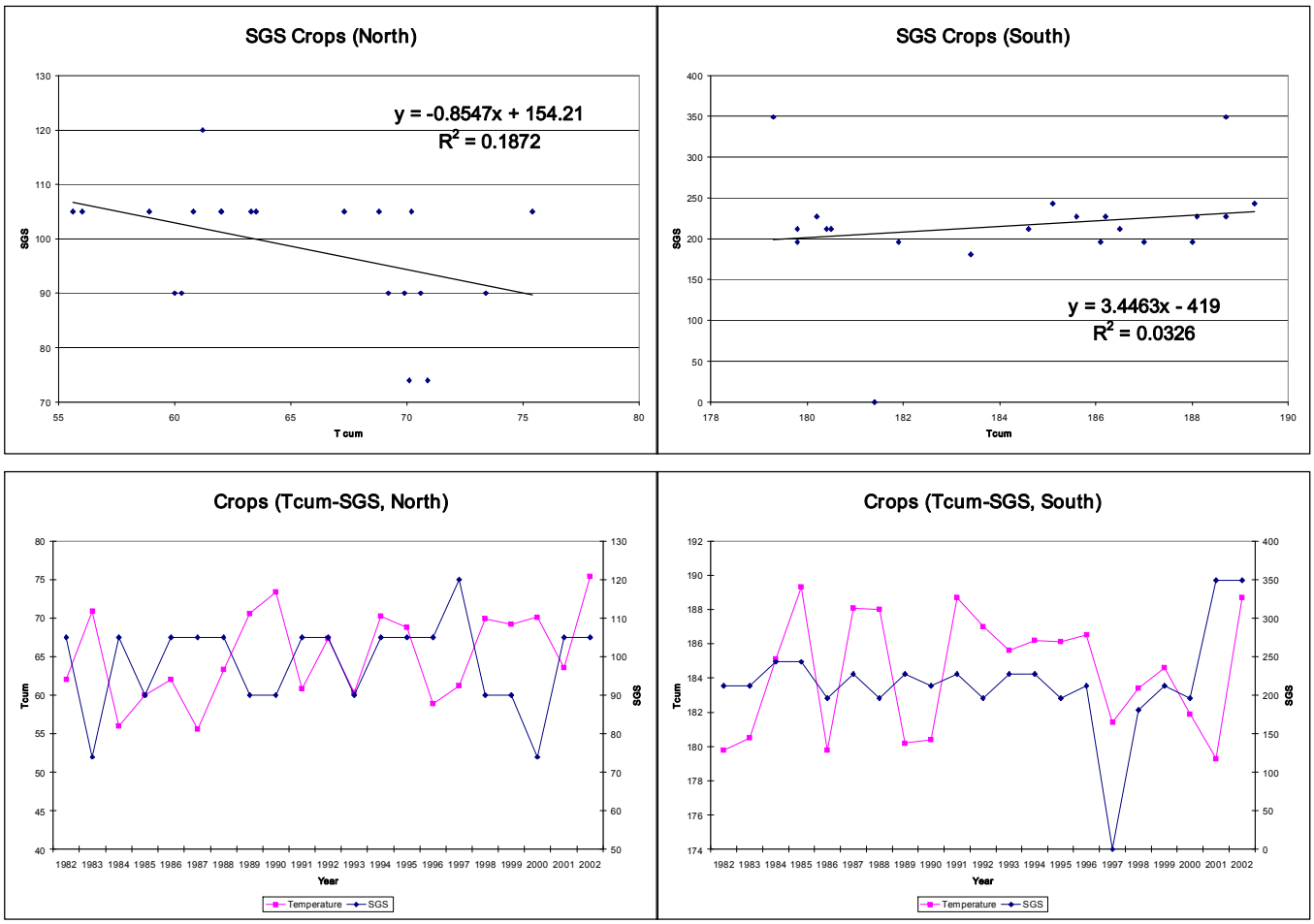

Figure 8-11. Crops SGS vs. Cumulative Temperature for North and South points.

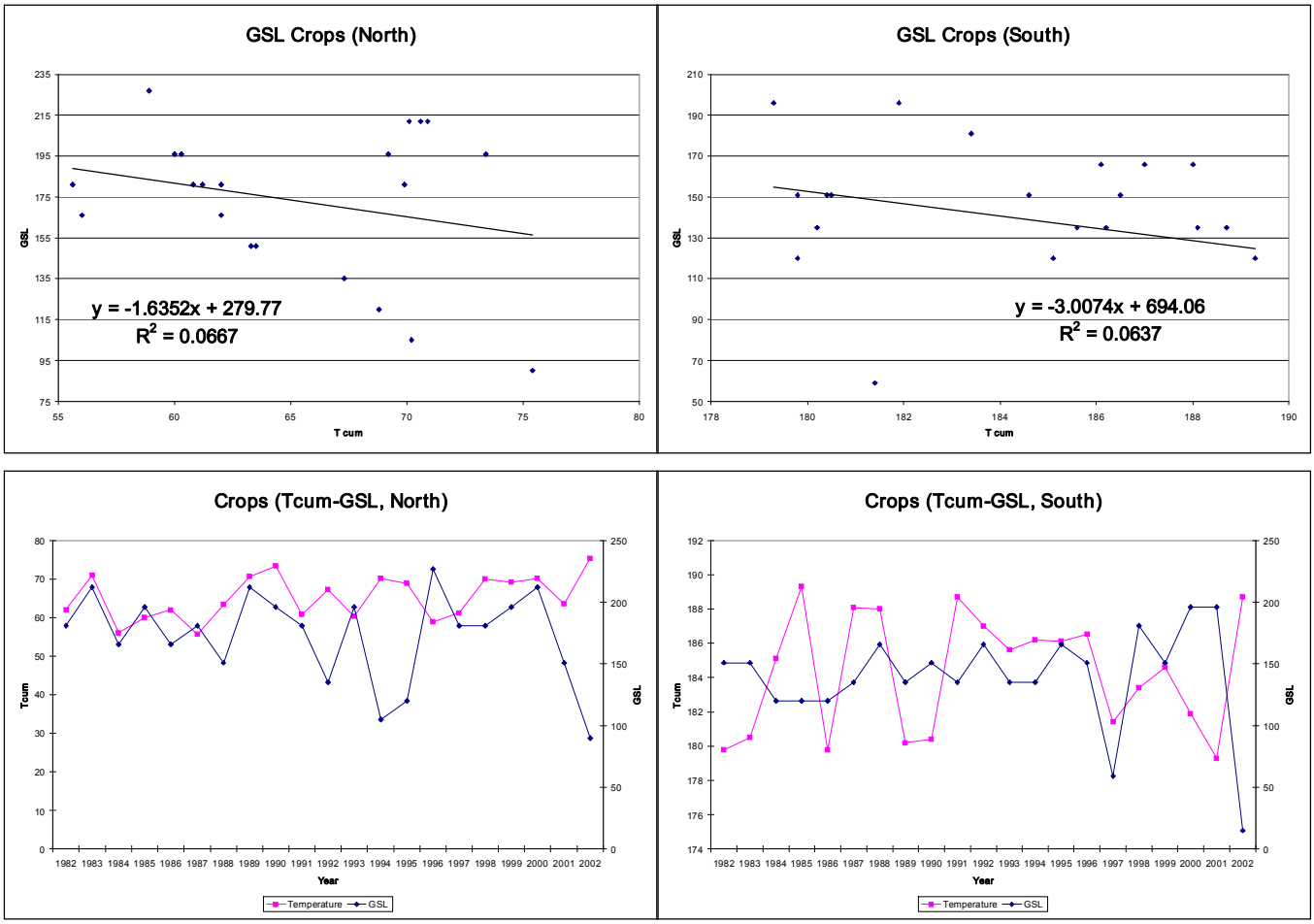

Figure 8-12. Crops GSL vs. Cumulative Temperature for North and South points.

Regression	Sample	R^2	Slope	Intercept	Pearson Correlation
Phase-Tcum	Broadleaf Forest (N)	0.331	0.014	2.281	0.576
	Broadleaf Forest (S)	0.042	0.005	2.591	0.205
	Coniferous Forest (N)	0.167	0.019	2.078	0.408
	Coniferous Forest (S)	0.036	-0.05	3.262	-0.19
	Grasslands (N)	0.105	0.008	2.771	0.324
	Grasslands (S)	0.036	0.023	-3.944	0.189
	Crops (N)	0.631	0.015	2.146	0.795
	Crops (S)	0.244	-0.026	6.02	-0.494
GSL-Tcum	Broadleaf Forest (N)	0.103	2.253	17.407	0.32
	Broadleaf Forest (S)	0.097	-3.459	399.212	-0.311
	Coniferous Forest (N)	0.003	0.426	137.04	0.059
	Coniferous Forest (S)	0.209	-8.209	484.239	-0.457
	Grasslands (N)	0.0004	0.148	107.474	0.02
	Grasslands (S)	0.139	-7.02	1558.852	-0.373
	Crops (N)	0.067	-1.635	279.773	-0.258
	Crops (S)	0.064	-3.007	694.064	-0.252
SGS-Tcum	Broadleaf Forest (N)	0.268	-2.329	240.595	-0.518
	Broadleaf Forest (S)	0.066	1.175	41.61	0.258
	Coniferous Forest (N)	0.004	-0.592	145.13	-0.07
	Coniferous Forest (S)	0.079	6.042	-59.275	0.282
	Grasslands (N)	0.119	-1.443	164.659	-0.344
	Grasslands (S)	0.132	-14.519	3139.42	-0.363
	Crops (N)	0.187	-0.855	154.208	-0.433
	Crops (S)	0.032	3.446	-419.005	0.181

Table 8-1. Regression summary of all land cover types vs. cumulative temperature